PHILOSOPHICAL TRANSACTIONS OF THE ROYAL SOCIETY A
MATHEMATICAL, PHYSICAL & ENGINEERING SCIENCES

Ice accretions on high–voltage conductors and insulators and related phenomena

Masoud Farzaneh

Phil. Trans. R. Soc. Lond. A 2000 **358**, 2971-3005
doi: 10.1098/rsta.2000.0692

10.1098/rsta.2000.0692

Ice accretions on high-voltage conductors and insulators and related phenomena

By Masoud Farzaneh

NSERC/Hydro-Québec/UQAC Industrial Chair on Atmospheric Icing, 555 boulevard de l'Université, Chicoutimi (Québec), Canada G7H 2B1
(farzaneh@uqac.uquebec.ca)

This paper proposes to survey a good part of the research work accomplished to date on the atmospheric icing of conductors and insulators in the presence of high voltage, with emphasis laid on the studies carried out at the University of Québec in Chicoutimi. The review covers laboratory testing and mathematical modelling.

The role of several electrical parameters, such as electric field strength and polarity, corona discharge, water droplet charge and ionic wind velocity, on the structure and amount of ice accretion on high-voltage conductors, is discussed.

Concerning the icing of insulators, the initiation of electrical discharge on the ice surface, the formation of local arcs along the air gaps and their development to a flashover arc along the insulators are discussed. Basic experiments on the role of several major parameters relating to ice accretion, insulator characteristics and voltage type and polarity, on the maximum withstand voltage of short insulators, are also discussed. Finally, several measures for improving the withstand voltage of insulators are briefly recalled.

Keywords: atmospheric icing; phase conductors; ground cables; high voltage; corona discharge; flashover arc

1. Introduction

In cold regions of the world, accretion of ice from the supercooled drops and droplets encountered in freezing rain, drizzle and in-cloud icing is a serious problem in electrical power systems. Mechanical and electrical effects are found on both overhead-conductor systems and on fixed installations such as outdoor stations.

Recent icing events in Québec and Ontario, in January 1998, illustrate very clearly the disastrous socio-economic consequences of damage to electrical power systems caused by atmospheric icing. In Québec, over one million customers, representing approximately one-half of the population of this Canadian province, were without power for periods of 3–30 days. Material damage was also substantial: several hundreds of miles of transmission, subtransmission and distribution lines were destroyed. The cost of network restoration, including reconstruction of the failed structures, has been estimated at nearly one billion Canadian dollars. Social cost may have exceeded three times that amount (Hydro-Québec Committee of Experts 1998).

Several different phenomena and their consequences are the result of atmospheric ice deposits on power network equipment.

(i) Freezing fog can stabilize insulator surface pollution into a thin (greater than 0.1 mm) ice layer, leading to, in severe cases, electrical flashover failure upon melting (Chisholm *et al*. 1996).

(ii) Under windy conditions, conductors covered with as little as 2 mm of asymmetrical ice may develop galloping. High-amplitude gallop, from the coupled vertical and torsional motion of conductors, reduces the air gap clearances between conductors, occasionally leading to flashover, and repeated interruptions of supply to customers (Havard & Pon 1998, 1990; Jones 1993).

(iii) Moderate (10–30 mm) accretion of ice on electrical insulators can lead to flashover, both during the icing period and later during a melting period, at electrical stresses well below 100 kV per metre (Wu *et al*. 1996; Farzaneh & Drapeau 1995; Phan & Matsuo 1983; Cherney 1980; Fujimura *et al*. 1979; Watanebe 1977; Kawai 1970; see also Sugawara *et al*. 1993; Shu *et al*. 1991; Vuckovic & Zdravkovic 1990; Lee *et al*. 1977; Schneider 1975).

(iv) Sudden ice shedding of moderate ice accretion, due to a number of possible mechanisms, causes mechanical shocks that sometimes lead to major mechanical damage to power network equipment (Roshan Fekr *et al*. 1998; Larcombe *et al*. 1991; Druez *et al*. 1990; Su & Hu 1988).

(v) Excessive ice accumulation of more than 50 mm, together with wind effects, also causes static mechanical damage to the conductors themselves, and to hardware, insulators and towers (Wareing & Bracey 1998; Goia & Balan 1996; Vuckovic *et al*. 1996; Tymofichuk 1986).

The occurrence of the above-mentioned phenomena, their degree of intensity and their effects depend on two main factors. First, the topographical, meteorological and environmental conditions establish the intensity, nature and duration of icing events. Second, important mechanical, thermal and electrical characteristics of the power system equipment to withstand these effects include insulator type, size and configuration, conductor size and composition, span length, tower strength and flexibility, load current, electric field strength, nature and polarity, and pollution levels on the equipment and in the accreted and melting ice.

Due to the number of physical phenomena and electrical factors acting simultaneously on individual supercooled drops and droplets, the determination of ice characteristics (density, structure, shape, etc.) and the amount of ice accreted on high-voltage equipment, as the origin of all the related phenomena and their consequences, is rather complex. Observations of ice deposits grown naturally on high-voltage equipment, such as conductors and insulators, are rather limited, so that very few data are accessible in the presently available literature. However, climate room experiments, involving essentially conductors and insulators submitted to high voltage, show that density and other characteristics of ice can be altered under energized conditions (Farzaneh & Laforte 1991, 1992, 1994; Teisseyre & Farzaneh 1990; Phan *et al*. 1983; Phan & Laforte 1981).

For the purpose of delimiting the review of research progress covered by the present paper, the phenomena caused by ice accretion on power network equipment, and their consequences, can be divided into two main categories. First, mechanical, relates to the increase in static and dynamic loads such as wind and iceloads, ice shedding, galloping and other types of vibrations in the presence of ice and wind, and their effects and consequences. Second, electrical, refers to events caused by the presence of high voltage, its variation and consequent electrical discharges. Flashover on iced insulators (Wu *et al*. 1996; Farzaneh & Drapeau 1995; Phan & Matsuo 1983; Cherney 1980; Fujimura *et al*. 1979; Watanebe 1977; Kawai 1970; see also Sugawara *et al*. 1993; Shu *et al*. 1991; Vuckovic & Zdravkovic 1990; Lee *et al*. 1977; Schneider 1975), short-circuit caused by decrease in clearance, changes in structure, amount and shape of ice (Farzaneh & Laforte 1991, 1992, 1994; Teisseyre & Farzaneh 1990; Phan *et al*. 1983; Phan & Laforte 1981), corona-induced vibration (Farzaneh 1986, 1992; Farzaneh & Teisseyre 1988; Farzaneh & Phan 1984), audible noise (Comber *et al*. 1982; Chartier *et al*. 1970), radio interference (Comber & Nigbor 1982) and, finally, their effects and consequences, are examples of this category.

In the past, investigation of the mechanical aspects has far outweighed that of electrical considerations. The main reason for such gaps in research is the fact that the problems, inconvenience and, especially, long-duration power interruptions caused by electrical phenomena are less frequent than those attributed to mechanical failure. Also, the electrical phenomena involve dynamic changes in electric field, corona discharge and partial and flashover arcs in various intricate combinations of geometric shapes and environments (insulating materials, air, liquid water, ice and metal electrodes, etc.), making the analysis of such phenomena rather complex.

A scope that would include only the electrical phenomena is still too ambitious for a single paper. Thus we will limit ourselves here to the electrical phenomena, and their consequences, related to ice accretion on two major power network elements: high-voltage conductors and insulators. In particular, the paper aims to review the progress in research dealing with the influence of electric field and corona discharge on the structure of ice accumulated on high-voltage conductors, and with flashover on ice-covered insulators. Special emphasis will be placed on the research conducted at the University of Québec in Chicoutimi.

2. Icing of high-voltage conductors

(*a*) *Generality*

A typical three-phase overhead transmission or distribution line is an energy corridor feeding the various electrical loads via conductors. In the case of transmission lines, depending on the voltage level, one or more conductors comprise a phase. The phase conductors are insulated from each other and from the tower, using suspension and tangent insulator strings. The overhead neutrals are electrically in contact with the tower and, therefore, grounded. The neutral cables shield the phase conductors against lightning and carry harmonic and power-system fault currents. Neutral cables are normally much smaller in diameter than conductors. The conductors are, in general, bare, to allow for efficient heat dissipation. While the relative variation of the electric field at the surface of phase conductors is small, the current transmitted by a line varies largely and even, in some cases, changes direction.

As concerns atmospheric ice conditions, several factors, such as geometrical position, torsional stiffness and absence of electric field and current, distinguish the icing of neutral cables from that of phase conductors. A relatively large number of icing models covering wet-snow, glaze and rime accretion on conductors and cables have been developed over the past years. The *Proceedings of the International Workshop*

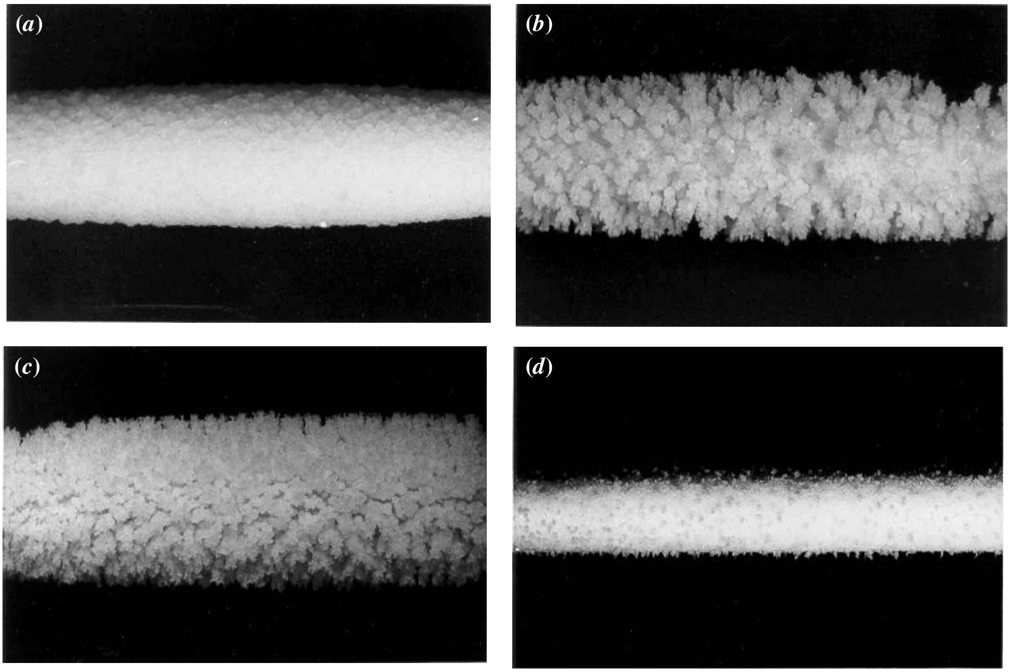

Figure 1. Visual appearance of ice accretions.

on Atmospheric Icing of Structures (IWAIS) are among the rich literature sources which cover almost all aspects of icing and most of the icing models developed. Several books have also been published on the subject; the most recent being by Poots (1996). Moreover, in this issue of *Philosophical Transactions*, the paper written by Makkonen provides a good review of significant papers on ice models.

As the influence of electrical parameters, such as electric field and corona discharge, on the icing of conductors has not been considered extensively in the past, the first part of the present paper aims to discuss the influence of these parameters on the physical and structural aspects of ice accretion on high-voltage conductors.

(*b*) *Influence of electric field on ice accretion on high-voltage conductors*

Several studies carried out on ice accretion on high-voltage conductors (Farzaneh & Laforte 1994; Teisseyre & Farzaneh 1990; Phan *et al.* 1983; Phan & Laforte 1981) show that the physical appearance of ice is closely related to the electric field strength at the surface of the conductors and to the polarity of applied voltage.

(i) *Physical aspect of ice accretion*

Figure 1 shows the visual aspects of ice accreted with no voltage applied (figure 1*a*), and with alternating (figure 1*b*), positive (figure 1*c*) and negative (figure 1*d*) applied fields of 15 kV cm^{-1} (Farzaneh & Laforte 1994). The conductor used was a soft aluminium cylinder, 3.15 cm in diameter, placed along the axis of a cylindrical mesh cage, 1 m in diameter. The experiments were carried out in a cold room, at a temperature of −10 °C. The mean conductivity of the tap water used to feed the nozzles

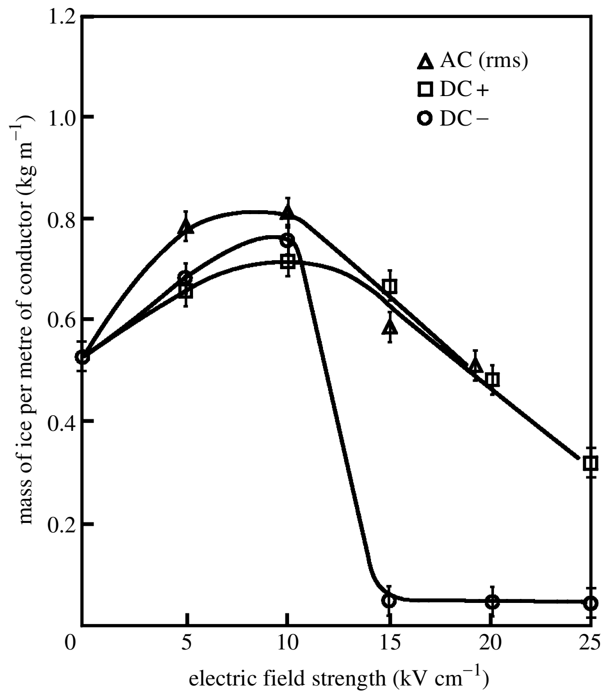

Figure 2. Weight of ice deposited per metre of conductor under energized conditions.

was *ca.* 55 μS cm^{-1} at 21 °C, the volume-median diameter of supercooled droplets *ca.* 40 μm, and the intensity of ice accretion for these experiments *ca.* 2.1 g m^{-2} s^{-1}, with no electric field applied.

In the absence of an electric field (figure 1*a*), the type of ice deposited was hard rime with small protuberances on its surface. In the presence of an electric field, these protuberances grow like trees with thin lateral feathery branches (figures 1*b*–*d*). When the electric field is positive (figure 1*c*), ice trees and side branches appear to be more numerous and thinner than those grown in an AC field (figure 1*b*). When the voltage is negative (figure 1*d*), the trunks of the ice feathers are even thinner than those observed under AC and DC+ voltage.

(ii) *Amount and density of ice accretion*

Figure 2 shows the weight of ice per unit length of cylinder as a function of electric field strength at the surface of the cylinder for AC, DC+ and DC− applied voltage (Farzaneh & Laforte 1994). The duration of ice accretion, under the same conditions, was 2 h. For all three cases, it may be observed that the weight of accreted ice first increases with electric field strength up to 10 kV cm^{-1}, then sharply decreases.

The most interesting results, which were obtained for a negative electric field above 15 kV cm^{-1}, indicate that the amount of ice accreted is almost negligible. Under AC and DC+, the decrease in weight of ice accretion with the increase in electric field strength, is much smaller than that measured under DC−.

Figure 3 shows the mean density of the ice accreted on the cylinder as a function of DC and AC electric field strengths (Farzaneh & Laforte 1994). The results show

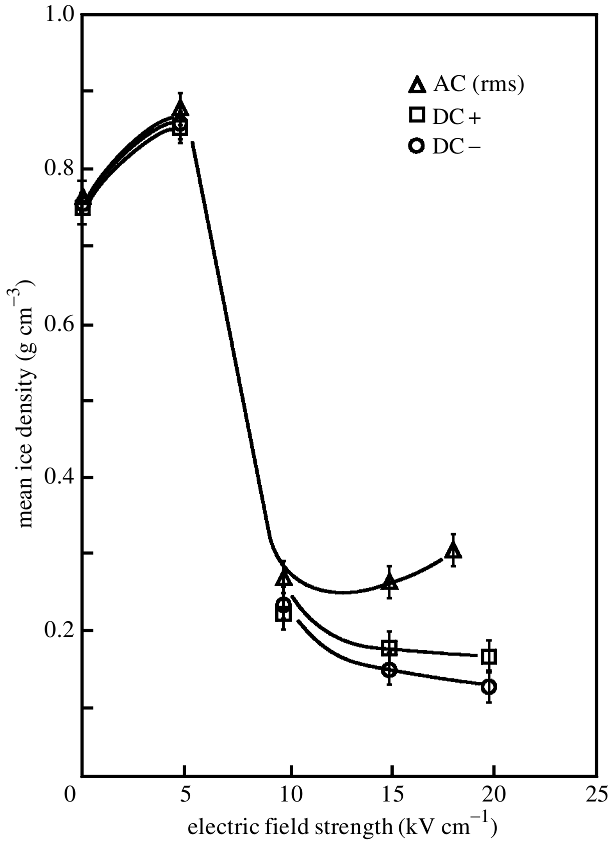

Figure 3. Mean density of ice deposits under energized conditions.

that ice density first rises under energized conditions up to 5 kV cm^{-1}, then decreases sharply as electric field strength increases.

(iii) *Structural parameters of ice*

In a collaborative project between the University of Québec in Chicoutimi, the University of Savoy, France, and Atomic Energy of Canada, efforts were focused on understanding the possible effects of an electric field on the structural parameters of ice grown under energized conditions (Farzaneh *et al*. 1996, 1997*d*).

In these experiments, the specific ice samples were made through the accretion of very fine supercooled droplets, 15 μm in volume-median diameter, of high isotopic purity heavy water (D_20), on the surface of a soft steel conductor. The conductor, 1.6 cm in diameter, was placed along the axis of a metallic cylindrical cage, 11.7 cm in diameter. The entire ice-accretion process was carried out in a cold chamber at a temperature of *ca*. −12 °C.

Neutron diffraction measurements on the ice samples were made on the DUALSPEC diffractometer at the Chalk River Laboratories of AECL Research, Canada. Before the neutron experiments, the samples were cooled to liquid nitrogen temperature, ground into fine powder and finally placed in thin-walled cylindrical vanadium cans. Measurements of lattice parameters a and c (Farzaneh *et al*. 1996, 1997*d*) were taken at -48 °C.

For this first attempt to determine what happens to the structure of ice grown in energized conditions, analysis of the data revealed small but significant effects on the unit cell volume. Lattice parameters a and c showed values *ca.* 0.08% higher for ice grown under an electric field strength of -15 kV cm when compared with the values obtained under non-energized conditions. With an electric field of $+15$ kV cm^{-1}, parameters a and c showed a change of the same magnitude, but of the opposite sign. Changes to the relative position of oxygen and deuterium atoms were less significant when the ice was grown under the influence of an electric field. Even if it is possible to understand the change of unit volume cell by considering the role of the electric field in the positioning of deuterium atoms, the relationship to voltage polarity will likely be far more difficult to interpret. Further studies are needed to answer some of these basic questions.

(*c*) *Discussion on the effects of electric field*

The presence of an electric field at the surface of high-voltage conductors is at the origin of several phenomena. Under freezing conditions, the electric field can induce dipoles of charge on droplets. It can also cause corona discharge at the tip of water droplets and ice asperities. In turn, corona discharge causes ions to collide with the droplets, thus charging them. Corona discharge is also at the origin of ionic wind generation. Additionally, during corona discharge either ions or electrons, depending on voltage polarity, bombard the surface of ice. In the following sections the effects of these parameters on ice accretion will be discussed.

(i) *Droplets charge by polarization*

The electric charge carried in each hemisphere of a droplet with a given radius, r, moving at distance, d, from the surface of a high-voltage conductor placed at the centre of a cylindrical cage is obtained as follows (Phan & Mansiaux 1975):

$$q_0 = \frac{12\varepsilon_0 U}{\ln(R_2/R_1)}\left(d \ln \frac{d}{d-r} - r\right), \tag{2.1}$$

where R_1 and R_2 are, respectively, the conductor and cylindrical cage radii, and U is the voltage applied to the centred conductor. For an electric field of 15 kV cm^{-1}, and a droplet size $r = 20$ μm, moving at 1 cm from the conductor, the calculated value of the charge is 6.4×10^{-16} C. This polarization charge is relatively small. However, at the ice protuberances (see figure 1), the electric field is enhanced so that the polarization becomes more efficient at those sites. Polarized droplets become attracted to the collector, regardless of polarity. This can explain the increased accretion of ice at 5 kV cm^{-1}, below which there is almost no corona discharge (Farzaneh & Laforte 1994). Even if the polarization process induces a force of attraction, regardless of voltage polarity, it seems to be a little more efficient under AC voltage, as more ice is accumulated than under DC voltage (see figure 2).

(ii) *Droplet charge from ion collisions*

The onset of corona discharge in laboratory icing of an energized conductor was observed visually and audibly. The electric field was slightly above 5 kV cm^{-1}, at

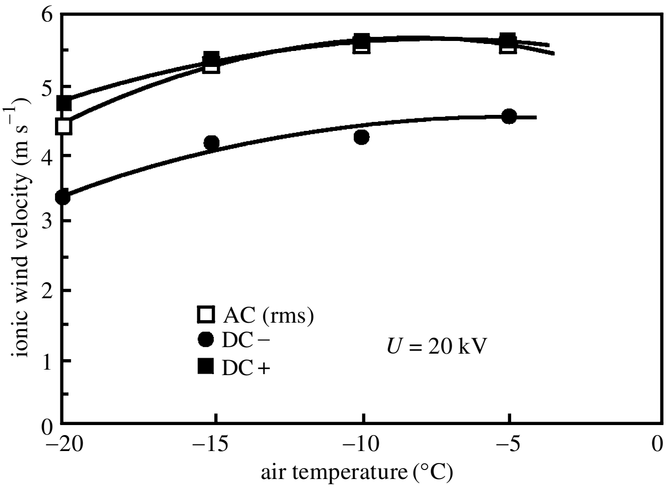

Figure 4. Ionic wind velocity versus air temperature for DC−, DC+ and AC.

both negative and positive polarities (Farzaneh & Laforte 1994). As corona discharges are particularly concentrated at the tips of the ice trees and branches, ions collide with droplets and give them an electrical charge. The polarity of the charge on water droplets is the same as that of the energized conductor. The maximum charge, q_s, a water droplet of a given radius r can acquire in an ionized field F is obtained from (White 1962):

$$q_s = \frac{3\varepsilon_r}{\varepsilon_r + 2} 4\pi\varepsilon_0 r^2 F, \tag{2.2}$$

where ϵ_r and ϵ_0 are the electric constants of water and air permittivity, respectively, and F is the undisturbed field, that is, the field removed from the particles or the discharge zone. For an applied field of 15 kV cm^{-1}, the undisturbed field 1 cm from the conductor is *ca.* 10 kV cm^{-1}. The maximum charge of droplets with a radius of 20 μm is equal to *ca.* 1×10^{-13} C. The relatively high value of the electric charge imparted by an ionized field reduces the impact velocity of the droplets and collection efficiency. Regarding the polarity effect, even if the maximum repulsive force is the same under both positive and negative polarities, the number of negatively charged droplets is expected to be about four times that of positively charged ones (Farzaneh & Laforte 1994). The ionization process could explain the sharp decrease in the amount of ice accumulated, especially at high electric field strengths. For a high negative electric field, due to the higher rejection of water droplets, this decrease in the amount of ice is more significant than it is for DC+.

(iii) *Effects of ionic wind*

During corona discharge, the ions created are accelerated by the electric field. Their momentum is transferred through collisions with molecules of the ambient gas, giving them motion from the tip of the asperity toward the environment. In the case of atmospheric ice accumulated on high-voltage conductors, the velocity of ionic wind near the asperities of ice influences the impact velocity of supercooled droplets, changing their collection efficiency. This will also affect heat transfer and, therefore, the cooling time of droplets. Wind velocity near an ice cone was measured in a previous study (Teisseyre & Farzaneh 1990). Figure 4 shows the ionic wind velocities as a function of air temperature on the axis of an ice cone, at a distance of 21 mm (Teisseyre & Farzaneh 1990). It may be observed that at a constant voltage (20 kV in this case) the ionic wind velocity in DC− is found to be in the area of 20–28% lower than the 5.5 $\mathrm{m\,s^{-1}}$ measured under DC+ and AC voltage. From the results, it is possible to estimate the velocity of droplets affected by ionic wind. Velocity is reduced considerably, changing the heat transfer, ice deposit temperature and density of ice accretion (Farzaneh & Laforte 1994).

(iv) *Bombardment of ice asperities*

During corona discharge, the surface of the ice on the conductor is bombarded by positive ions under a negative field, and by the electrons under a positive field (Teisseyre & Farzaneh 1990). The total kinetic energy, W_b, due to bombardment can be estimated from the number of mono-charged particles impinging on the ice surface, the ratio J/e (J being the corona current and $e = 1.6\times10^{-19}$ C), the particle mass m, its mobility μ and the electric field F, applied to the following equation:

$$W_\mathrm{b} = \frac{J}{e} m\mu^2 F^2. \tag{2.3}$$

The calculation shows that, at a constant voltage, the energy due to the bombardment of ice asperities is about three times higher under negative polarity than it is under positive polarity (Farzaneh & Laforte 1994; Teisseyre & Farzaneh 1990). This difference was confirmed by measuring the loss in ice volume under DC−, DC+ and AC (Farzaneh & Laforte 1994; Teisseyre & Farzaneh 1990). It was observed that, at constant voltage and temperature, the loss in volume was greater under DC− than under DC+. The results confirmed that bombardment of ice asperities is effectively more intense by positive ions than by electrons. These bombardments contribute to a warming of the ice surface, especially on asperities, resulting in superficial melting. However, this heat is removed from the iced surface by convection and evaporation, which are proportional to the difference between air and ice temperatures.

(*d*) *Influence of transmitted current*

The current I_L transmitted by a three-phase transmission or distribution line is calculated as follows:

$$I_\mathrm{L} = \frac{P}{\sqrt{3} V_\mathrm{L} \cos\varphi}. \tag{2.4}$$

In this equation, P is the electrical transmitted power, V_L the voltage between two phase conductors and $\cos\varphi$ the power factor. Supposing R to be the resistance per unit metre of each conductor at operating conditions, power loss as Joule effect per unit metre may be calculated from the following:

$$P_\mathrm{j} = R I_\mathrm{L}^2 = \frac{RP^2}{3V_\mathrm{L}^2 \cos^2\varphi}. \tag{2.5}$$

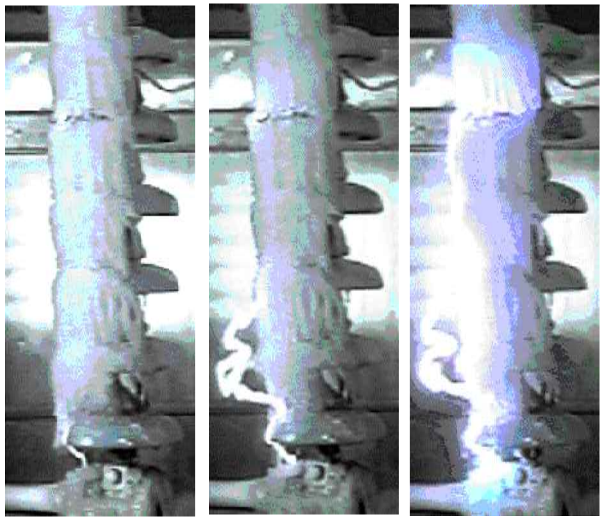

Figure 5. Presence of air gaps and arc development.

Depending on conductor characteristics, and meteorological and icing conditions, this heat loss may have either a small or large impact on the amount and/or type of ice accretion. Consequently, it is important to consider the influence of current on the amount of ice accretion on phase conductors, using mathematical ice models. This work should be supported by field and laboratory studies. Such research is presently in progress at the Industrial Chair CIGELE in Chicoutimi.

3. Insulation flashover under icing conditions

(a) Generality

Power network outdoor insulators are the devices that support, separate and/or contain the high-voltage conductors. Insulators have both mechanical and electrical functions. Requirements for the mechanical strength of insulators are determined by the load conditions to which they will be submitted in the field. However, this aspect of insulators will not be considered in the present paper. From the electrical point of view, the insulators should withstand electrical stress with low probability of failure and flashover under the permanent and transient conditions to which they are subjected. In practice, there exist no ideal insulators, that is to say non-conductive insulators. The main reason is that outdoor insulators are subjected to the effects and consequences of environmental and meteorological conditions. Typically, a pollution layer containing inert mineral matter, electronic-conductive dust like carbon or metal oxides, soluble salts and water, is formed on the surface of the insulators. In cold regions, atmospheric ice constitutes another type of pollution, from the point of view of insulation and in addition to such a contaminant layer. Due to the freezing process, corona discharge products and the presence of other contaminating substances, the surface of the ice deposited on insulators is normally highly conductive (Rizk 1995; Farzaneh & Melo 1990, 1994; Sugawara *et al*. 1993; Nasser 1972; Lambeth 1971; Forrest 1969). Under such conditions, leakage current is established and creates heating effects, electrochemical products of electrolysis and electrical discharges. This situation sometimes leads to flashover; the complete bypassing of electrical insulation by a breakdown path that is sufficiently ionized to maintain an arc which then short-circuits the phase conductor.

A very large number of papers has been published regarding pollution-caused flashover. A survey of several broad reviews of flashover due to pollution, published over the past 30 years, may be found in Rizk (1995), CIGRÉ WG 33.04 (1979), IEEE Working Group on Insulator Contamination (1979), Nasser (1962, 1972), Lambeth (1971) and Forrest (1969).

As opposed to the effects of pollution on the electrical performance of insulators, very little has been done in the area of flashover of ice-covered insulators. However, the socio-economic impact of power outages due to insulator flashover has motivated several utility companies and researchers from various countries to investigate this problem. Short reviews of the principal investigations have been completed recently (Farzaneh & Kiernicki 1997*a*, 1995). The following sections cover the progress of research on ice-covered insulator flashover.

(*b*) *Flashover mechanisms on ice-covered insulators*

Generally, the ice accretion along the insulators is not uniform, as several parts of the insulators are free of ice; these zones are referred to as air gaps. They are caused by the heating effect of partial arcs or by ice shedding from the insulators, brought about by several mechanisms during or after ice accretion. In general, it is agreed that the presence of a water film on the surface of the ice is necessary for flashover to occur. This water film can be caused by a number of processes: wet ice accretion; condensation; heating effect of leakage current; partial arcs; or, in many cases, by the rise in air temperature or sunshine. The high conductivity of the water film means that voltage drops occur essentially across the air gaps. This phenomenon is caused by the rejection of impurities from the solid part toward the liquid portion of drops or droplets during solidification, and by pollution of the water and ice surface by the products of corona discharge. If the stress along the air gaps is high enough, several violet arcs will appear across them. Under sufficient electrical stress, arcs propagate along the ice surface, forming a white arc. Finally, when the white arc reaches a certain length, flashover occurs suddenly. Figure 5 shows the air gaps and the different stages of a flashover process along an insulator string artificially covered with ice. It should be noted that all the mechanisms involved in the initiation of discharges, and their transition to arc propagation on the ice surface, are not known. More research is needed to better understand these processes.

MATHEMATICAL, PHYSICAL & ENGINEERING SCIENCES
THE ROYAL SOCIETY A
PHILOSOPHICAL TRANSACTIONS OF

(*c*) *Fundamental aspects of discharge initiation and arc propagation on the surface of ice*

Although a relatively large number of publications and reports have focused on the flashover performance of ice-covered insulators, only a few have concentrated on the fundamental aspects of discharge on ice surfaces, or in the air gap between two ice-formed electrodes. These include Bandel (1951), Jordan & Saint-Arnaud (1976), and Griffiths & Latham (1974), who studied corona discharge on ice needles. For their part, Phan *et al.* (1974) studied the evolution of corona discharge from a water drop during its transition from liquid to solid phase, and vice versa. The authors found that corona activity decreases considerably when the drop freezes. Sato *et*

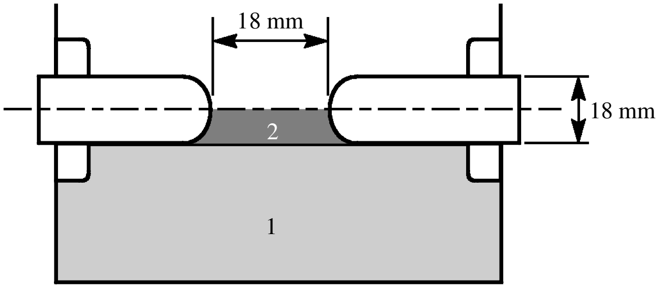

Figure 6. Vertical cut of the ice model at rest.

al. (1989) carried out a number of flashover tests on an iced plate sprayed with a solution of NaCl. They compared flashover on iced plates for various types of ice deposits. Using two metallic hemispherical capped rods, separated by an ice surface, Farzaneh *et al*. (1998*a*, 1999*a*) studied the flashover voltage of the ice surface under DC, AC and lightning impulse voltage. These studies led to a better understanding of the role of ambient air and freezing water conductivity on ice surface flashover. Very recently, a research project was undertaken, with the aim of understanding the discharge initiation mechanisms on ice surfaces and their evolution to flashover arc. Particularly, ultra-high-speed photographs, taken with a streak camera (Farzaneh *et al*. 1999*b*) and a high-speed frame camera (Zhang & Farzaneh 2000), were used to determine the initiation of visual discharge and its development, and the fundamental characteristics of arc, such as radius and propagation velocity. These data were also used to construct models to predict flashover voltage on ice surfaces. The following sections consider these aspects.

(i) *Discharge initiation and development*

Ultra-high-speed photographic observation of discharge initiation and development to flashover on ice surfaces, using metallic hemispherical capped electrodes half imbedded in ice (figure 6), was recently carried out at the University of Québec in Chicoutimi (Farzaneh *et al*. 1999*b*), within the framework of the Industrial Chair on Atmospheric Icing of Power Network Equipment (CIGELE).

Figure 7 shows the streak images of the discharge development on the surface of ice made from de-ionized water, at air temperatures of −20 and 0 °C. In the first case, at −20 °C (figure 7*a*), the surface of ice was dry, while in the second case, at 0 °C (figure 7*b*), a water film was present on the ice surface. For a dry and clean ice surface, the first visible discharge activity occurred in front of the anode and, some 5.5 ns later, a second area of discharge activity became visible in front of the cathode. Both partial discharges extended towards the central area between the electrodes, until breakdown occurred. When a water film was present on the surface of the ice (figure 7*b*), the visible discharge activity started at some point on the ice surface and breakdown followed very quickly. Similar results, not presented here, were obtained with highly conductive dry-surfaced ice (Farzaneh *et al*. 1999*b*). These first studies of discharge initiation and development on ice surfaces show the major role the presence of a water film and high surface conductivity play on the development of flashover arc on ice surfaces. Further studies are planned to better understand the

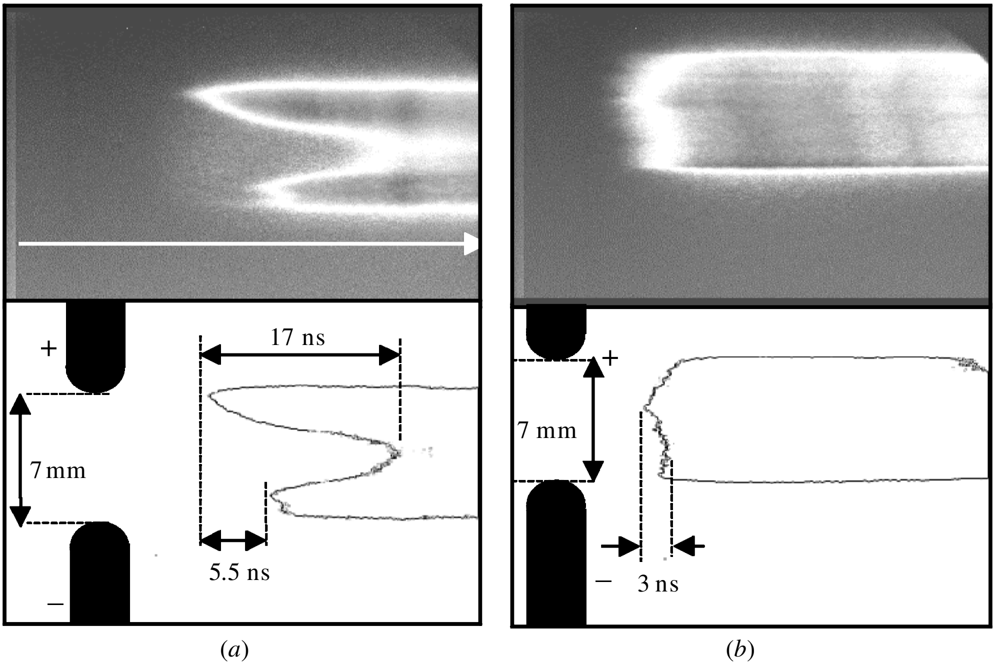

Figure 7. Streak images of the discharge development on the surface of the ice. (*a*) Clean ice with dry surface ($T = -20$ °C, $\sigma = 1$ µS cm^{-1}). (*b*) Clean ice with water film on the surface ($T = 0$ °C, $\sigma = 1$ µS cm^{-1}).

effects electrical charging of the ice surface can have on the initiation of discharges, and the conditions of their development into flashover arc.

(ii) *Fundamental behaviour of AC and DC arcs on ice surfaces*

Arc propagation velocity

Using a high-speed camera and a triangular ice sample, fundamental arc parameters and behaviour, such as root radii under AC and DC voltage, were investigated (Zhang & Farzaneh 2000; Farzaneh *et al*. 1997*c*). Figure 8 shows the ice sample made from the freezing of water with a conductivity of 80 µS cm^{-1}, as well as the test circuit used for the experiments. The 1 cm air gap made at the top of the ice sample simulated the air gaps found on ice-covered insulators and made possible the initiation and propagation of arc on the ice surface. The flashover tests were carried out by establishing a high voltage, slightly higher than the minimum flashover voltage of the ice surface, between two metallic electrodes fixed at the top and bottom of the ice sample (Zhang & Farzaneh 2000; Farzaneh *et al*. 1997*c*). All the flashover tests were carried out at 0 °C, on the samples placed vertically in a climate room. In the course of the flashover tests, a high-speed frame camera was used to record the flashover process. This camera made it possible to measure the arc root and its propagation velocity, as well as to record simultaneously the voltage and corresponding current of the arc.

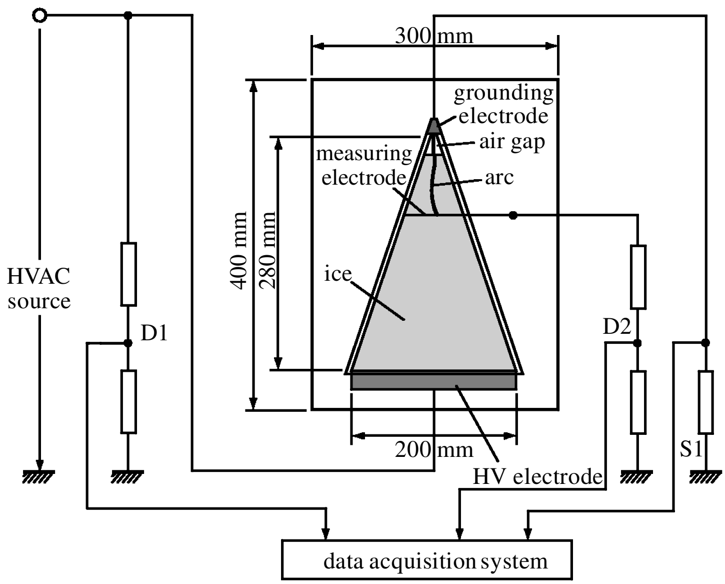

Figure 8. Sample and test circuit: D1, D2, voltage divider; S1, current shunt.

It was found that during the flashover process, the arc may propagate in two different ways: (i) over the ice surface, through the air, hereafter called an outer arc; or (ii) inside the ice, hereafter called an inner arc. Parts (*a*) and (*b*) of figure 9 show the inner and outer arc propagation processes respectively. A large number of observations reveal that propagation of the arc, outer or inner, occurs at random. The propagation process of both outer and inner arcs is in general completed in two stages. The first stage begins with the formation of the arc, with an initial length equal to 5% of the length of the ice between the two electrodes (L), and corresponds to the air gap length, and ends when arc length reaches *ca.* 45–60% of L. At this stage, the arc is formed mostly outside the ice, in the air, and extends relatively slowly. During the second stage, arc propagation velocity increases suddenly until flashover occurs. The maximum arc velocity is reached just before flashover. At this stage, the arc may be formed either in the air or inside the ice.

Table 1 shows the propagation velocities of positive, negative and alternating arcs. These results show that arc propagation velocity on ice surfaces, especially during the first stage, is relatively slower than that obtained on a polluted surface (Ghosh & Chatterjee 1996; Li *et al.* 1990).

Relation between arc root radius and leakage current

The radius of arc root is one of the major factors determining the flashover voltage of the ice surface (Rizk 1981). It depends not only on the environmental conditions, such as air temperature, humidity and pressure, but also on the leakage current through the arc. For DC arcs, the relationship between the arc root radius and the leakage current can be determined by recording and analysing the arc propagation process and the corresponding leakage current. Under AC voltage, the arc radius varies with the leakage current during the half cycle of applied voltage. However, the

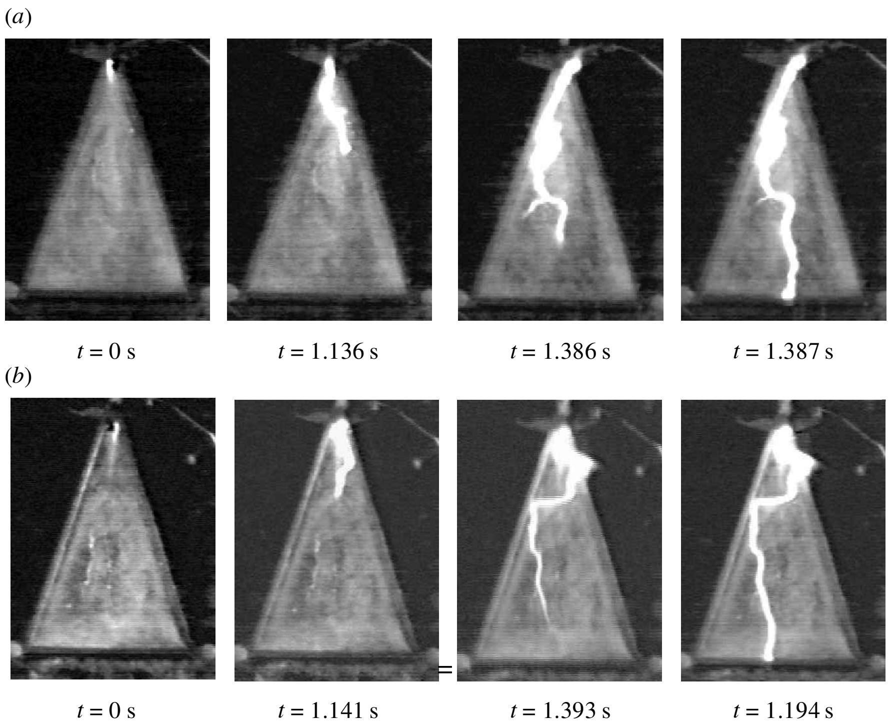

Figure 9. Arc propagation process on ice surfaces under DC.

Table 1. *DC and AC arc propagation velocities*

arc type		arc propagation velocity ($m\ s^{-1}$)		
		first stage	second stage	maximum value
positive arc	outer	0.05 to 0.3	20 to 50	≈ 100
	inner		3 to 7	≈ 50
negative arc	outer	0.05 to 0.3	35 to 60	≈ 100
	inner		10 to 20	≈ 50
AC arc	outer	0.04 to 0.15	16 to 30	≈ 440
	inner		2 to 7	≈ 260

arc radius and the leakage current reach their peak values concurrently. Therefore, after recording and analysing these peak values, the relationship between the arc root radius, r, and the leakage current, I_m, can also be determined. For the purpose of that particular study, using a triangular ice sample (see figure 8), changing the conductivity of the water used to form the ice samples served to vary the leakage current during flashover.

Figure 10 shows an example of positive arc radius as function of leakage current. It may be observed that, as leakage current increases, the arc root radius also increases.

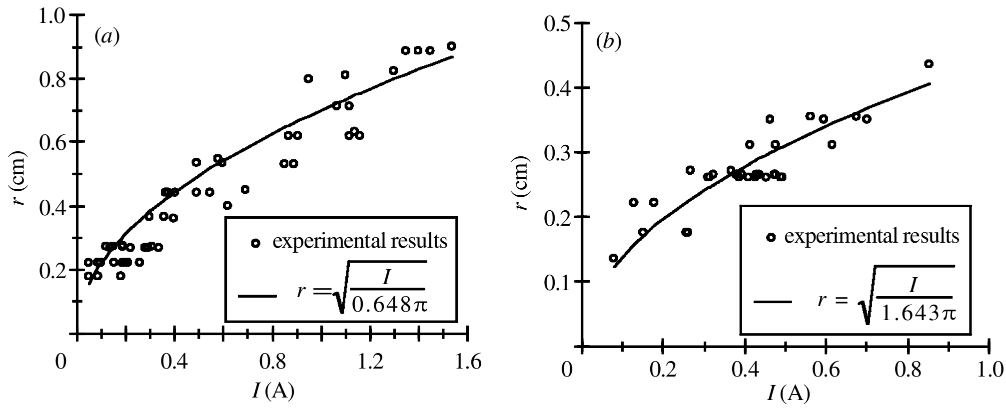

Figure 10. Radius of positive arc as a function of leakage current. (*a*) Outer arc, (*b*) inner arc.

Table 2. *Inner and outer arc radii as functions of leakage current*

arc type		arc radius
positive arc	inner arc	$r = \sqrt{I/1.643\pi}$
	outer arc	$r = \sqrt{I/0.648\pi}$
negative arc	inner arc	$r = \sqrt{I/1.759\pi}$
	outer arc	$r = \sqrt{I/0.624\pi}$
alternating arc	inner arc	$r = \sqrt{I_m/2.439\pi}$
	outer arc	$r = \sqrt{I_m/0.875\pi}$

Applying the regression method to the experimental results, the relationship between arc root radius, r, and leakage current, I, for both inner and outer DC and AC arcs, was determined and is presented in table 2.

The difference between the values of inner and outer arcs for a given value of leakage current is probably caused by the difference in environment temperature between inner and outer arcs, that of inner arcs being lower due to surrounding ice, while outer arcs burn in the air.

(iii) *Arc modelling on ice surfaces*

In previous works (Zhang & Farzaneh 2000; Farzaneh *et al.* 1997*c*, 1998*b*), a model based on the method used for polluted insulating surfaces was used to calculate the DC and AC flashover voltage of ice-covered insulators. The general equation for this model is expressed as follows:

$$V_m = V_e + A I_m^{-n} X + I_m R(X), \tag{3.1}$$

where V_m is the applied voltage, V_e the electrode voltage drop, X the arc length, I_m the leakage current, $R(X)$ the residual resistance, and A and n the arc constants.

Under AC voltage, the electrode voltage drop, V_e, can be neglected and included in the drop of arc (Farzaneh *et al.* 1997*c*; Rizk 1981; Claverie & Porcheron 1973).

Table 3. *Electrode voltage drop, V_e, and arc and re-ignition constants*

type of voltage	V_e (V)	A	n	k	b
DC−	527	84	0.77		
DC+	799	209	0.45		
AC	0	205	0.56	1118	0.53

Also, V_m (in volts) and I_m (in amps) represent the peak values of applied voltage and leakage current.

In addition, under AC conditions the re-ignition conditions must be satisfied in order for the arc to keep burning. These re-ignition conditions are expressed by the following equation:

$$V_m = \frac{kx}{I_m^b}, \tag{3.2}$$

where k and b are the re-ignition constants.

Using a triangular ice sample (see figure 8), the constants of arc, A and n, for AC and DC arcs, as well as the re-ignition constants k and b, were determined (Zhang & Farzaneh 2000; Farzaneh *et al*. 1997*c*, 1998*c*) and are presented in table 3.

To the best of our knowledge, these models for AC and DC voltage are the first and only ones that can predict the critical flashover of industrial insulators in the presence of ice. The application of these models to the calculation of industrial insulator performance under icing conditions will be discussed later.

(*d*) *Evaluation of critical flashover voltage of ice-covered insulators*

The critical flashover voltage of ice-covered insulators may be determined experimentally or with mathematical models. However, both methods, and particularly modellization, are still in the development phase.

(i) *Experimental methods*

The experiments for evaluating the electrical performance of insulators under icing conditions may be done in laboratories or at outdoor test stations. Laboratory tests are based on the principle of growing artificial ice on insulators (Farzaneh & Drapeau 1995; Sklenicka *et al*. 1983; Schneider 1975) and then evaluating the flashover performance, using a predetermined test procedure. Historically, outdoor stations used the cold temperature at night for ice accretion and the flashover tests were done in the morning when the ice started to melt because of sunshine or a rise in temperature (Schneider 1975).

While outdoor stations allow for the evaluation of the electrical performance of insulators at full scale and at reasonable costs, the results are not precise. This is mainly due to the fact that neither the ice nor the meteorological parameters, which largely influence the characteristics of ice accretion on insulators, can be controlled during the tests. Proper control of such parameters can only be achieved in climate rooms. However, most existing climate rooms are too small for testing extra high voltage (EHV) insulators at full scale.

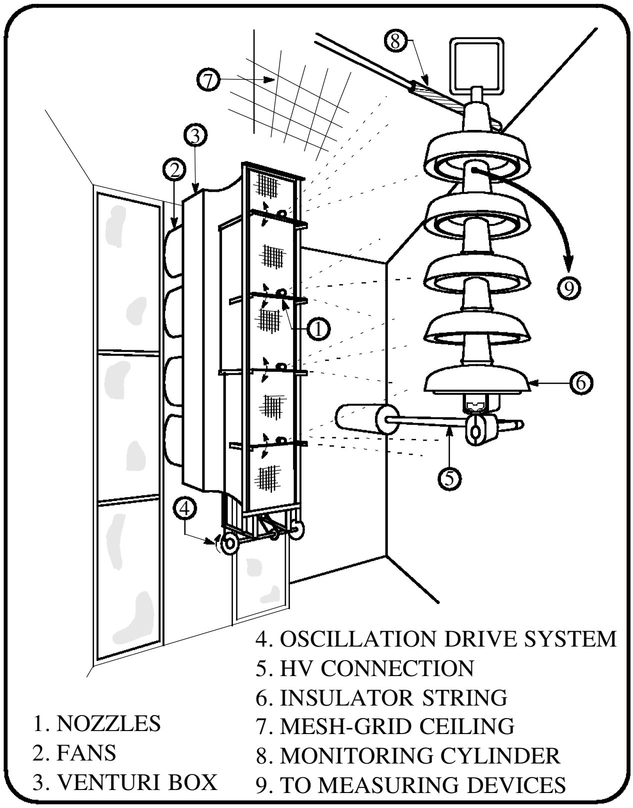

Figure 11. Climate room and facilities.

The following sections concern the experimental procedure for laboratory evaluation of insulators, as carried out at the University of Québec in Chicoutimi (Farzaneh & Kiernicki 1997*b*; Farzaneh & Drapeau 1995).

Ice-accretion methods and facilities

The climate room at the High-Voltage and Atmospheric Icing Laboratory of the University of Québec in Chicoutimi measures $6.6 \times 5.1 \times 3.7\ m^3$ (figure 11). The room is equipped with a spray-and-wind generation system, as well as a high-voltage bushing, to achieve accumulation of various types of ice from supercooled droplets, and to carry out flashover tests on insulators up to 1 m long.

The spray system consists of a set of air-atomizing nozzles mounted on a vertical support. The system oscillates on a vertical plane. De-ionized water, of which the conductivity is adjusted by adding sodium chloride, feeds the sprays. To generate a relatively uniform wind, fans are mounted in two stages in a tapering box equipped with a diffusing honeycomb panel.

Adequate instruments make it possible to control and measure the environmental and icing conditions and parameters. Air temperature is controlled by a proportional integral differential (PID) system, with a precision of $\pm 0.2\ ^\circ C$. A suspended mesh grid facilitates rapid temperature exchange and minimizes the temperature gradient in the climate room. The liquid water content (LWC) of the air containing the supercooled droplets is measured by the single-cylinder method, from the weight of ice accreted on a small-diameter cylinder. The median volume diameter of the supercooled droplets is measured by exposing a glass slide, coated with a solution of Collargol, to a flow of water droplets for a short time period (Godard 1960). The samples are then examined under a microscope and the mean volume diameter of these droplets is determined from the average diameter of *ca.* 1000 droplets. The density of ice is determined by weight and volume measurements. The thickness of ice on testing equipment is controlled by a monitoring cylinder 3.8 cm in diameter and rotating at 1 rpm (Farzaneh & Kiernicki 1997*b*; Farzaneh & Drapeau 1995).

By means of a high-voltage bushing, AC or DC high voltage is applied to the testing equipment during icing and flashover tests (see figure 11). The AC high-voltage system consists of a 240 kVA, 120 kV transformer and a 240 kVA regulator. The overall short-circuit current of the HVAC system is *ca.* 28 A at the maximum operating voltage of 120 kV. DC high voltage is obtained by using a thyristor-controlled system, which ensures a dynamic voltage drop of output voltage less than 5% for a 0.5 A load current.

Voltage application and testing methods

To the best of our knowledge, there is no established standard method for evaluating the flashover performance of insulators under atmospheric icing conditions. Recently, a CIGRE Task Force (TF.33.09.09) initiated the preparation of Guideline Applications and looked to publish two Electra review papers suggesting such testing methods and proposing prevention methods. Hopefully, these publications will soon be available.

Standard methods facilitate the comparison of results from different laboratories and testing sites, thus allowing for a better understanding of the influence of atmospheric ice on the flashover performance of various outdoor insulator types. Standards will also allow us to compare the flashover performance of various types of insulators presently used in cold climates and help transport and distribution energy companies select the most adequate. In addition, the effects of the parameters of individual insulators on their flashover performance under icing conditions could be studied, leading to the establishment of design criteria for insulators for use in atmospheric icing conditions.

Recently, within the framework of a collaborative research project financed by the Natural Sciences and Engineering Research Council (NSERC) of Canada and Hydro-Québec, two methods to determine the critical flashover voltage of insulators were developed at the University of Québec in Chicoutimi (UQAC). These methods are described in the following paragraphs.

MATHEMATICAL, PHYSICAL & ENGINEERING SCIENCES
PHILOSOPHICAL TRANSACTIONS OF THE ROYAL SOCIETY A

Maximum withstand voltage

This method was based on, and developed from, the method described in the standard IEC507 (International Electrotechnical Commission 1991) for determining the maximum withstand voltage of contaminated insulators. Voltage application methods on insulators during icing, melting and flashover testing appear in figure 12, and may be summarized as follows. After the icing period, t_{i}, at an air temperature, T_{i},

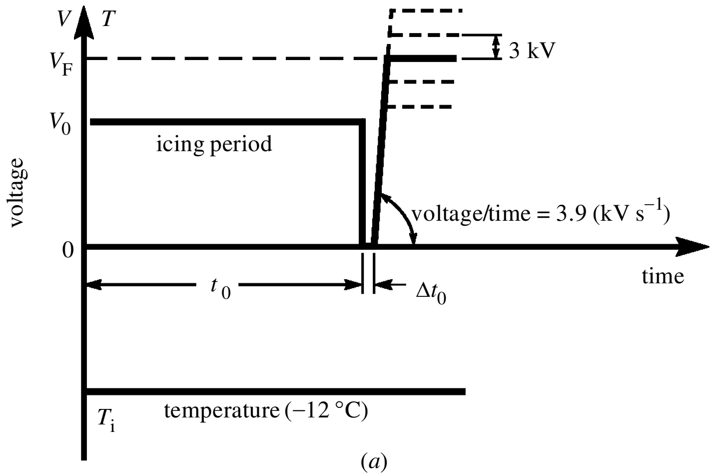

(a)

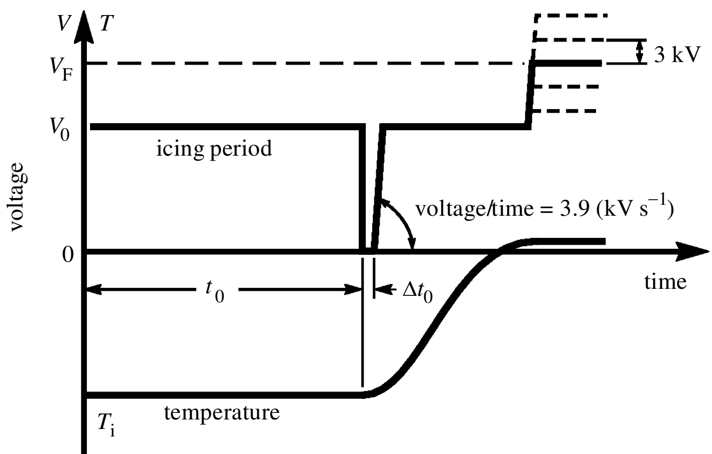

(b)

Figure 12. Voltage application method during (*a*) icing, (*b*) melting, and (*a*), (*b*) flashover testing.

equal to $-12\,^\circ$C, and during which the service voltage, V_0, was applied to insulators, the spray nozzles and the voltage were turned off. After a short period, Δt_0 (*ca.* 2.5 min), the insulators were photographed while test preparations were completed. After this short period, water was still dripping from the insulators.

At this point, two possibilities were offered. In the first instance, voltage was re-applied to the insulators and increased rapidly (3.9 kV s^{-1} at UQAC) by automatic control, until the estimated value of flashover voltage, V_F, was reached (figure 12*a*). The second possibility (figure 12*b*) calls for the service voltage, V_0, to be re-applied and the ambient temperature to rise at a given mean rate from T_i to *ca.* $+1\,^\circ$C, thus causing the ice to melt and a water film to form at its surface. Generally, the melting period starts when the dew point of the air in the chamber reaches $0\,^\circ$C. During the melting period, if it is judged necessary, the voltage V_0 may be either raised or lowered, or even, in some cases, turned off completely. In these experiments, the voltage was increased from V_0 to V_F (figure 12). In either case, with or without a melting period, when voltage V_F was reached, the maximum withstand voltage, V_{WS}, was determined using a method similar to that described in the standard IEC507 (International Electrotechnical Commission 1991), in which voltage is raised in steps of 5% from the initial voltage V_F. Each flashover test was performed for one instance of ice accumulation on the insulators. Maximum withstand voltage was considered the maximum level of applied voltage at which flashover did not occur for a minimum of three tests out of four, under similar experimental conditions. For each withstand test, the insulators were kept under test voltage, V_F, for a period of 15–30 min. The minimum flashover voltage, V_{MF}, corresponded to a voltage level 5% higher than V_{WS}, at which flashover occurs twice out of a maximum of three tests.

50% withstand voltage

This method was also based on, and developed from, the method described in the standard IEC507 (International Electrotechnical Commission 1991). In a way similar to the first method, after ice accretion and photography, and, after a melting period, in some cases, voltage was again applied to the insulators and increased until the estimated value of flashover voltage, V_F, was reached. The 50% withstand voltage was then determined using the up-and-down method. The voltage step was similar to that described in the first method. Each test was performed for one instance of ice accumulation. A test was considered as withstand if no flashover occurred for a period of 15–30 min under testing voltage. The insulators were subjected a minimum of 10 'useful' tests. The first 'useful' test is that which yields a different result from the preceding test.

Figure 13 shows the flashover performance of six units of porcelain standard insulators, 254 mm diameter on 146 mm vertical spacing, covered with 2 cm (measured on the monitoring cylinder) of wet-grown ice (glaze with icicles), using the two methods mentioned above (Farzaneh & Kiernicki 1997*b*). The ice was not submitted to a melting period in these experiments.

(ii) *Application of the mathematical model*

The electrical performance of insulators under icing conditions may be evaluated using mathematical models. However, to the best of our knowledge, the only mathematical models developed for this purpose are those introduced in the previous section of the present study (Zhang & Farzaneh 2000; Farzaneh *et al*. 1997*c*, 1998*c*).

In general, under atmospheric ice conditions, only the insulator surface facing the freezing precipitation is covered with ice, while the opposite side remains free of ice (Farzaneh & Drapeau 1995). Consequently, to calculate the 50% withstand voltage, the ice accumulated on insulators should be considered as a half cylinder. The residual resistance of the ice layer for the outer arc can therefore be expressed as follows (Farzaneh *et al*. 1997*c*; Wilkins 1969)

$$R(x) = \frac{1}{2\pi\gamma_e}\left[\frac{4(L-x)}{D+2d} + \ln\left(\frac{D+2d}{4r}\right)\right], \tag{3.3}$$

where γ_e is the surface conductivity of the ice layer, L and D the length and diameter of the insulator string, respectively, d the thickness of the ice layer, and r the arc root radius, calculated from table 2.

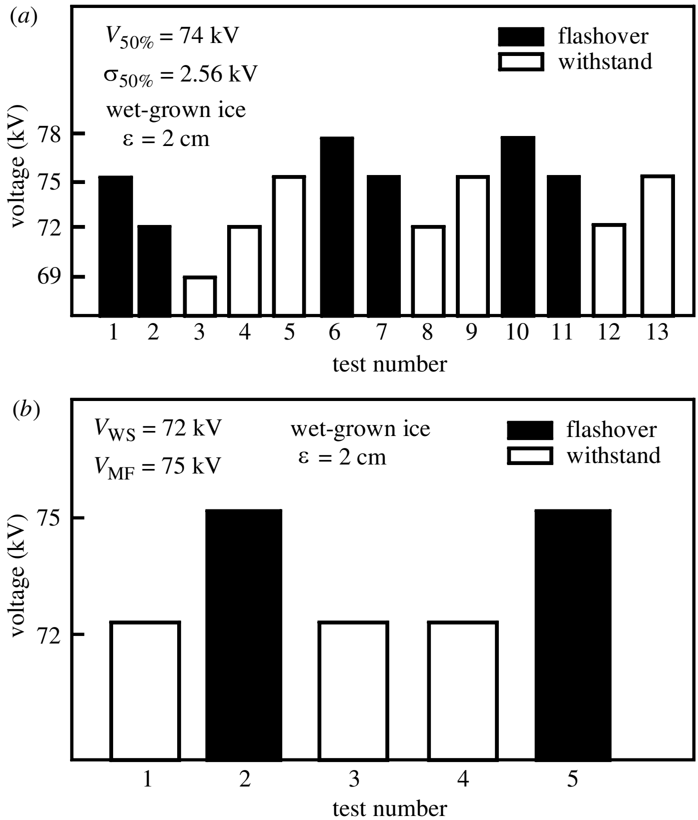

Figure 13. Test results using the (*a*) 50% withstand and (*b*) maximum-withstand methods.

The arc constants, A and n, and the re-ignition constants, k and b, have previously been calculated and presented in this paper. The ice surface conductivity, γ_e (measured in μS), can be calculated from the following equations

$$\gamma_e = 0.0599\sigma + 2.59 \quad \text{for DC}-, \tag{3.4}$$

$$\gamma_e = 0.082\sigma + 1.79 \quad \text{for DC}+, \tag{3.5}$$

$$\gamma_e = 0.0675\sigma + 2.45 \quad \text{for AC}, \tag{3.6}$$

where σ (in $\mu S\ cm^{-1}$) is the conductivity of freezing water, measured at 20 °C.

The mathematical model was used to calculate the 50% withstand voltage of a short five-unit string of IEEE insulators covered with 2 cm of ice and for different values of freezing water conductivity.

In order to validate the results of modelling, the 50% withstand voltage of insulators was measured experimentally (figure 14). The tests show good concordance between mathematical model calculations and experimental results. This model was also successfully applied to insulator flashover from 44 to 500 kV (Chisholm 1997). Refinement of the model, taking into account the effects of insulator length and shape, continues at CIGELE.

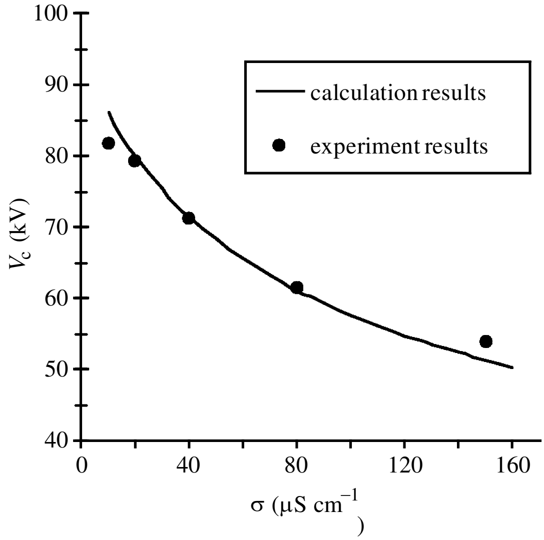

Figure 14. Calculated and experimental results of flashover voltage with five units of IEEE standard insulators.

(e) *Factors influencing flashover voltage of ice-covered insulators*

A number of factors and parameters influence the flashover voltage of insulators under icing conditions. These include: (i) the proper parameters of insulators such as dry arcing and leakage distances, the insulator diameter, profile and configuration, as well as the material covering the insulators; (ii) the ice parameters and atmospheric conditions, including ice type, amount, shape and distribution, the conductivity of freezing water, as well as air temperature, pressure, contamination and humidity; and finally (iii) voltage type and polarity.

(i) *Insulator parameters*

Dry arcing and leakage distances

For short insulators, several authors showed that the flashover voltage varies almost linearly with arcing distance (Kannus *et al*. 1988, 1998; Farzaneh & Kiernicki 1997*b*; Farzaneh & Drapeau 1995; Phan & Matsuo 1983). However, for long insulators, this relationship seems to be nonlinear (Sklenicka & Vokalek 1996; Su & Jia 1993). More research is necessary to establish a relationship between dry arcing distance and flashover voltage for long insulators. Figure 15 shows the linear variation of the maximum withstand voltage of one to six units of IEEE standard insulators covered with uniform wet-grown ice (Farzaneh & Kiernicki 1997*b*). The thickness of the ice on the monitoring cylinder was 2.0 cm.

Leakage distance on the flashover voltage of ice-covered insulators is influenced by icicle length, insulator precontamination, air humidity, air temperature variation and several other parameters. More research is necessary to clarify these effects. However, when the insulators are completely bridged with ice, the effect of dry arcing distance is more relevant.

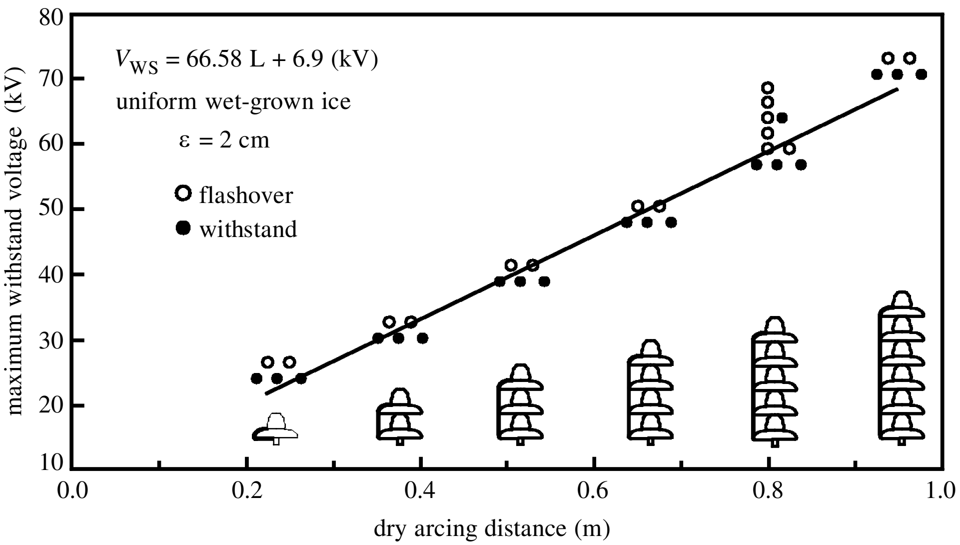

Figure 15. Maximum withstand voltage as a function of dry arcing distance of the insulator string.

Insulator diameter, profile, configuration and material

The amount of ice accretion on an object is proportional to the surface exposed to supercooled droplets. Consequently, under similar conditions, an insulator with a large diameter will accumulate more ice than a same-length smaller-diameter insulator. In terms of electrical performance, this means that large insulators will lose more of their leakage resistance than smaller ones. The larger insulators are therefore more prone to flashover under icing conditions, as suggested by Hydro-Québec service experience (Drapeau *et al.* 1996, confidential report). This is supported by the application of the mathematical model (Farzaneh *et al.* 1997*c*) to insulators 100 and 300 mm in diameter (Chisholm 1997).

Concerning the shed profile, insulators with a short shed spacing are more quickly bridged with icicles and, consequently, are more likely to flashover. Also, the configuration of insulators has an obvious effect on their flashover voltage. For example, with horizontal and V-string insulators, the possibility of ice bridging, and, consequently, flashover, is reduced when compared to vertical insulators. Conversely, parallel insulators separated by a short distance provide the possibility of ice accretion between the insulator strings, and to a reduction in withstand voltage.

Further research is necessary to determine the effects of surface material on the electrical performance of insulators under icing conditions.

(ii) *Icing parameters and atmospheric conditions*

Type and density of ice

The results of research as reported by several authors (Sugawara *et al.* 1993; Khalifa & Morris 1968) and of those carried out at UQAC (Farzaneh & Kiernicki 1997*b*, 1995; Farzaneh & Drapeau 1995; Farzaneh *et al.* 1992) show that both type and density of ice are the major factors influencing the flashover voltage of insulators.

Table 4. *Maximum withstand stress of insulators covered with wet-grown ice* ($s = 80\ \mu\mathrm{S\ cm}^{-1}$)

	E_{WS} (kV m^{-1})			
type of ice	IEEE	anti-fog	EPDM	post-type
wet grown	70	84	96	90
dry grown	> 197	> 197	> 197	> 197

EPDM = ethylene propylene, diene monomers.

Table 4 shows the results of an investigation on the effects of wet-grown ice (glaze with icicles) with a density of *ca.* 0.87 g cm^{-3}, and soft rime with a density lower than 0.3 g cm^{-3}, on the maximum withstand stress (E_{WS}) of different types of insulators (Farzaneh & Kiernicki 1995). These results show that wet-grown ice deposits are more dangerous than ice grown in a dry regime (soft rime in this study).

Amount of ice built up

The amount of ice on insulators is monitored in different ways. This includes measuring of the amount of ice (Shu *et al*. 1991, 1993; Yamazaki *et al*. 1993), length of icicles (Yamazaki *et al*. 1993; Sugawara *et al*. 1990; Fujimura *et al*. 1979; Renner *et al*. 1971), duration of the icing period (Erven 1988; Kannus *et al*. 1988; Charneski *et al*. 1982), and thickness of ice on a fixed (Wu *et al*. 1996) or rotating monitoring cylinder (Farzaneh & Drapeau 1995; International Electrotechnical Commision 1991; Phan & Matsuo 1983).

Figure 16 shows the relationship between the maximum withstand stress (E_{WS}), thickness of wet-grown ice on the monitoring cylinder, and corresponding weight of the ice per metre of IEEE insulator string (Farzaneh & Kiernicki 1997*b*). These results show that the E_{WS} of insulators decreases with an increase in ice thickness, up to 2.5 cm, and then remains constant. The critical value of ice thickness at which withstand voltage levels off varies with insulator type. The values of 2.0, 2.5 and 3.0 cm were, respectively, obtained for glass cap-and-pin (Phan & Matsuo 1983), EPDM (Farzaneh *et al*. 1994) and porcelain post-type insulators (Farzaneh & Drapeau 1995).

Ice distribution and shape

Due to melting and shedding, caused by several mechanisms, and in the presence of high voltage, some parts of the insulators remain free of ice (Wu *et al*. 1996; Farzaneh & Drapeau 1995; EPRI 1982). This non-uniform ice distribution along the insulators is the main cause for the nonlinear relation between the flashover voltage and length of long insulator strings.

The shape of ice and orientation of icicles, which depend mainly on wind velocity, are other parameters influencing the flashover of insulators. Strong winds tilt the icicles away from the wind, while they remain nearly vertical when subjected to light winds. As a result, the lowest maximum withstand voltage of vertical insulators is obtained when wind velocities are low (Farzaneh & Drapeau 1995; Farzaneh & Kiernicki 1995).

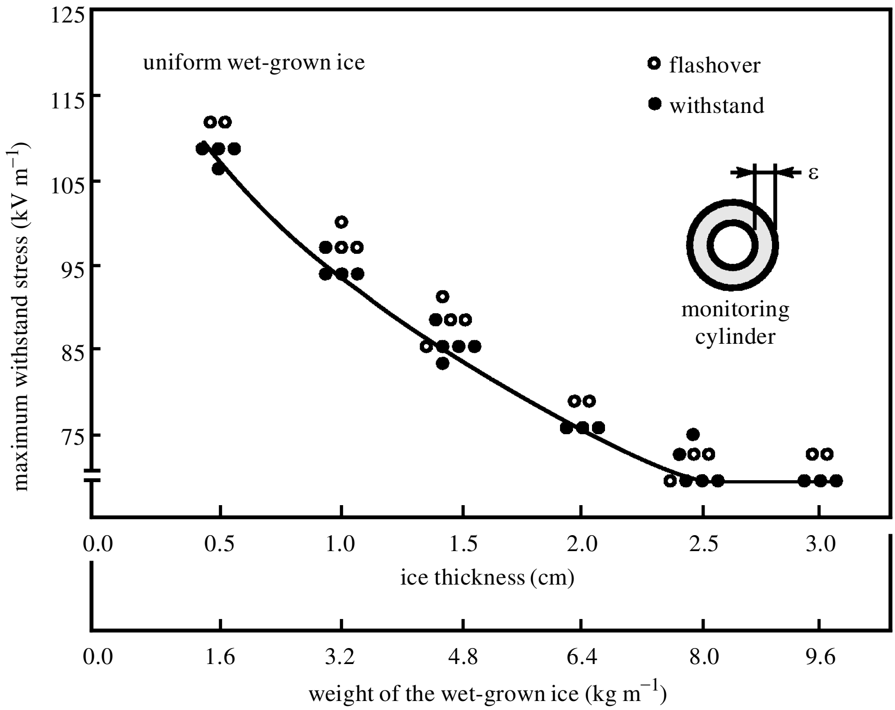

Figure 16. Maximum withstand stress per metre of IEEE insulators as a function of the ice thickness on the monitoring cylinder, and the corresponding weight of ice on 1 m of insulator string.

Freezing water conductivity

This major parameter considerably influences the flashover voltage of insulators. In general, the higher the conductivity, the lower the flashover voltage will be (Farzaneh & Kiernicki 1997*b*; Wu *et al*. 1996; Chisholm & Kuffel 1995; Farzaneh & Drapeau 1995; Fikke *et al*. 1994; Kannus *et al*. 1988; Phan & Matsuo 1983).

Figure 17 shows the decrease in the maximum withstand stress of a short string of IEEE standard insulators covered with wet-grown ice. The freezing water conductivity was varied and measured at 20 °C. The decrease in E_{WS} (kV m^{-1}) as a function of water conductivity under experimental conditions (Farzaneh & Kiernicki 1997*b*) can be expressed by the following power curve

$$E_{\mathrm{WS}} = 165.3\sigma^{-0.18}, \tag{3.7}$$

σ being expressed in μS cm^{-1} and measured at 20 °C.

However, in some cases, due to ice shedding, the increase in conductivity may lead to higher flashover voltage (Farzaneh & Drapeau 1995).

Rise in air temperature

The rise in air temperature from values under the freezing point to values around or above 0 °C causes the ice surface to melt. The formation of a water film, in general very highly conductive (Chisholm & Kuffel 1995; Farzaneh & Melo 1990,

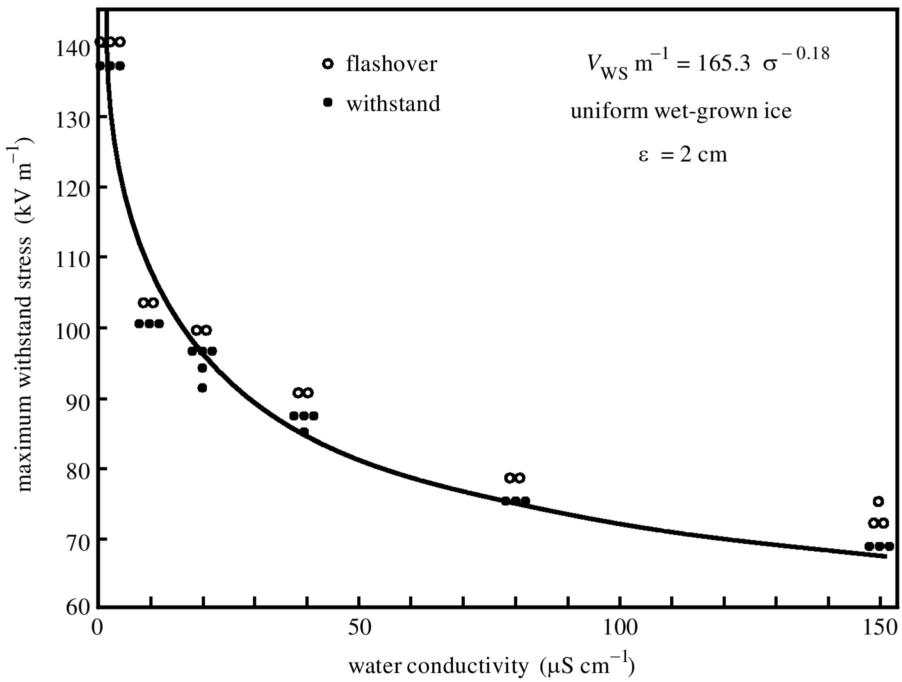

Figure 17. Variation of the maximum withstand stress of the insulators as a function of freezing water conductivity.

Table 5. *Maximum withstand stress* (E_{WS}) *versus rate of rise in air temperature* ($\Delta T/\Delta t$)

	E_{WS} (kV m^{-1})	
$\Delta T/\Delta t$ (°C h^{-1})	IEEE standard	composite EPDM
2.4	75.4	92.4
24	81.7	88.2

1994; Sugawara *et al*. 1993), at the ice surface, causes in turn an increase in voltage drop across the air gaps, and the formation of local arcs as a consequence. Under certain conditions, local arcs develop into a flashover arc along the whole insulator length.

The critical flashover voltage of insulators under melting conditions seems to depend on the rate of increase in air temperature (Soucy 1996; Farzaneh *et al*. 1995, confidential report). Table 5 shows the maximum withstand stress (E_{WS}) of a composite EPDM and the porcelain IEEE standard insulators under slow and fast ice melting conditions, as obtained at UQAC (Soucy 1996).

The above results show that while a relatively slow rise in air temperature, from −12 to +1 °C, at a rate of 2.4 °C h^{-1}, is most severe for porcelain IEEE standard insulators, rapid melting at 24 °C h^{-1} lowered the E_{WS} of the composite EPDM insulator tested (Soucy 1996).

Decrease in air pressure

At high altitudes, the electrical performance of insulators is not only influenced by atmospheric icing, but also enhanced by low air pressure (Farzaneh *et al*. 1997*a*, 1998*b*). The influence of air pressure on the critical flashover voltage of polluted insulators is generally considered by introducing an air density correction factor, K_{d}, which relates the critical flashover voltage, V, at any pressure, P, to the corresponding value, V_0, at standard sea level pressure, P_0,

$$V = K_{\mathrm{d}} V_0. \tag{3.8}$$

In general, the air density correction factor, K_{d}, depends on insulator profile, pollution severity and type of voltage. K_{d} may be derived from (3.9). For simplicity, the pressure ratio is considered to have already been corrected for temperature in this relation,

$$K_{\mathrm{d}} = \left(\frac{P}{P_0}\right)^m. \tag{3.9}$$

Exponent m is a constant and indicates the degree of influence of air pressure on critical flashover. This exponent depends, in general, on the type of voltage, insulator profile, pollution severity and even voltage application method (Meier & Niggli 1968). Using a triangular ice sample and also a short insulator, the values for m, while using DC and AC high voltage, were determined (Farzaneh *et al*. 1997*a*, 1998*b*). These results show that air pressure has an obvious influence on the minimum flashover voltage, V_{MF}, of tested objects. In some cases the results indicate that the reduction in the minimum flashover voltage could reach 40%, as ambient pressure decreased from 103.3 (sea level) to 30 kPa (9000 m) (Farzaneh *et al*. 1997*a*).

Insulator precontamination

In general, insulator precontamination depresses the critical flashover voltage of insulators under icing conditions (Chisholm *et al*. 1996; Soucy 1996; Chisholm & Kuffel 1995; Farzaneh *et al*. 1995, confidential report; Farzaneh & Melo 1994; Fikke *et al*. 1994; Fujimura *et al*. 1979; Udo *et al*. 1968). The effect of contamination on insulators becomes particularly important when water condensation takes place (Chisholm *et al*. 1996; Chisholm & Kuffel 1995). When this happens, any part of the surface of the insulator that is free of ice is wetted, which could promote insulator flashover if the critical situations are reached. The results of flashover tests on ceramic and non-ceramic insulators (Soucy 1996; Farzaneh *et al*. 1995, confidential report) showed that light contamination of 0.05 mg cm^{-2} could depress the flashover voltage of insulators by *ca.* 5% compared with the absence of precontamination. These results also show that with a higher precontamination, *ca.* 0.1 mg cm^{-2}, flashover voltage will decrease considerably. Flashover could then occur even during ice accretion.

(iii) *Voltage type and polarity*

Most of the research work on the electrical performance of insulators under icing conditions has been carried out under alternating voltage. However, a few authors carried out tests under switching impulse voltage (Udo *et al*. 1968) and direct voltage

Table 6. *Maximum withstand stress of a short string of IEEE standard insulators under artificial wet-grown ice*

type of voltage	E_{WS} (kV m^{-1})
DC+	86
DC−	71
AC	85

Table 7. *Comparison between the severities of ice and salt contamination*

ε (cm)	0.5	1.0	1.5	2.0	2.5	3.0
ESDD (mg cm^{-2})	0.02	0.04	0.07	0.13	0.15	0.15

(Farzaneh *et al*. 1997*b*; Farzaneh 1991; Renner *et al*. 1971). According to reference (Udo *et al*. 1968), the flashover voltage of a tested post-insulator stack under impulse voltage sometimes decreased as much as 50%, compared with dry and clean conditions.

As concerns DC flashover voltage, a series of tests carried out at the University of Québec in Chicoutimi (Farzaneh *et al*. 1997*b*; Farzaneh 1991) showed that the maximum withstand stress (E_{WS}) of a short string of IEEE standard insulators was *ca*. 17% lower under DC− than under DC+. Further tests revealed that the E_{WS} of insulators covered with ice are practically equal under DC+ and AC (table 6).

The thickness of ice on the monitoring cylinder for the above experiments was 1.5 cm.

(iv) *Comparison between effects of ice and contamination*

Although the mechanisms of flashover on insulators under pollution and ice conditions are different, the comparison between their effects in critical flashover voltage is possible. As reported in the previous section of the present paper, atmospheric ice, and especially wet-grown ice, decreases the withstand voltage of insulators considerably. The severity of ice depends particularly on freezing water conductivity and thickness of ice on the insulators. However, the presence of a water film on the surface of the ice, and that of air gaps, are the main factors that establish the critical conditions under which flashover occurs. In the case of polluted insulators, the formation of dry bands and the presence of wet zones on the insulator surface are the main causes of flashover. To evaluate the electrical performance of insulators under artificial pollution, the severity of the pollution layer is expressed in terms of the equivalent salt density deposit (ESDD). The higher this value is, the lower the withstand voltage will be.

A comparison between the effects of ice and contamination is shown in table 7 (Farzaneh & Kiernicki 1997*b*).

This comparison is made for the most severe type of ice, wet-grown ice, and a given freezing water conductivity of 80 μS cm^{-1}, measured at 20 °C. The thickness of ice, ϵ, reported in the table is as measured on a rotating monitoring cylinder. A given thickness was defined to be equivalent to a given value of ESDD when the minimum flashover or maximum withstand voltage of two short identical IEEE standard insulator strings, one covered with ice and the other contaminated and submitted to clean fog, are equal.

These results reveal that wet-grown ice accreted on a clean insulator string could have as much effect on the withstand voltage as moderate pollution, equivalent to an ESDD of 0.15 mg cm^{-2}.

(v) *Solutions for increasing reliability*

To the best of our knowledge, there exist almost no established insulator design criteria that take in account the effects of atmospheric icing. In the absence of more appropriate insulators with good electrical performance under icing conditions, many power transmission and distribution companies must accept the inconveniences related to flashover in the presence of ice, while some have proposed or adopted several measures for improving the withstand voltage of insulators (Chisholm *et al*. 1996; Sklenicka & Vokalek 1996; Wu *et al*. 1996; Sklenicka *et al*. 1983; EPRI 1982; Kawai 1970; Khalifa & Morris 1968). These measures include reducing the number of parallel insulators, using 'V' or horizontal strings (EPRI 1982), booster sheds (Sklenicka *et al*. 1983), insulators with alternating sheds, semiconductor glaze insulators (Chisholm *et al*. 1996) or corona rings (Wu *et al*. 1996) or, finally, lowering the operating voltage (Drapeau *et al*. 1996, confidential report; Khalifa & Morris 1968). These measures are proposed especially to prevent ice and icicle bridging, to make voltage distribution more uniform, or to decrease the electrical stress along the insulators. However, these methods have their inconveniences. For example, the use of booster sheds may interfere with natural washing, economic losses may be incurred in the case of semiconductor-glaze insulators and stability problems may occur with lower operating voltage. Moreover, the efficiency of each measure should be based on longer-term field experience under various icing and pollution conditions.

4. Conclusion

A review of the effects of atmospheric ice deposits, such as those formed from the impinging of supercooled droplets on high-voltage conductors and insulators, confirms that the presence of an electric field affects the structure, density and amount of ice accreted on conductors. Also, electric fields are at the origin of the initiation of electrical discharges and their development to flashover of iced insulators.

In general, and under certain conditions, the amount and density of ice deposits decrease with an increase in electric field at the surface of the high-voltage conductors. This decrease in amount and density is more pronounced under negative voltage than it is under positive and alternating voltage. The electrical charge of water droplets, the mode of corona discharge and the presence of ionic wind are several major parameters that cause such changes.

Concerning arc development on iced insulators, the presence of a highly conductive water film, causing zones of high electrical stress along the air gaps, is the major factor leading to flashover arc development under service voltage. Several major parameters related to ice, insulators, as well as the type and polarity of voltage, influence the critical flashover voltage of insulators under icing conditions.

This review reveals that further fundamental research is needed to understand the effects of electric fields on ice accretion where high-voltage conductors are concerned.

PHILOSOPHICAL TRANSACTIONS OF THE ROYAL SOCIETY A MATHEMATICAL, PHYSICAL & ENGINEERING SCIENCES

Also, it seems urgent that standard methods for evaluating the flashover performance of insulators under atmospheric ice conditions be put into effect. Additionally, more field studies and observations are necessary to establish the meteorological and environmental conditions which cause the insulators to flashover under icing conditions. Finally, it is also necessary to establish design criteria for insulators to be used on overhead power networks exposed to atmospheric ice accretion.

The author thanks Dr William A. Chisholm, from Ontario Hydro Technologies, for discussion and helpful suggestions. He also thanks the Natural Sciences and Engineering Research Council (NSERC) of Canada, as well as Hydro-Québec, for sponsoring several projects at the University of Québec in Chicoutimi, which are referred to in the paper.

References

Bandel, H. W. 1951 Corona from ice points. *J. Appl. Phys.* **22**, 984–985.

Charneski, M. D., Gaibrois, G. L. & Whitney, B. F. 1982 Flashover tests on artificially iced insulators. *IEEE Trans. Power Apparatus Sys.* **101**, 2429–2433.

Chartier, V. L., Shankle, D. F. & Kolcio, N. 1970 The Apple Grove 750 kV project: statistical analysis of radio influence and corona loss performance of conductors at 735 kV. *IEEE Trans. Power Apparatus Sys.* **89**, 867–881.

Cherney, E. A. 1980 Flashover performance of artificially contaminated and iced long-rod transmission line insulators. *IEEE Trans. Power Apparatus Sys.* **99**, 46–52.

Chisholm, W. A. 1997 Discussion to Farzaneh, Zhang & Chen 1997. *IEEE Trans. Power Delivery* **12**, 334–335.

Chisholm, W. A. & Kuffel, J. 1995 Performance of insulation coatings under contamination and icing conditions. In *Canadian Electrical Association, Electricity 95 Conference, Transmission Section, March 1995, Vancouver.*

Chisholm, W. A. (and 12 others) 1996 The cold-fog test. *IEEE Trans. Power Delivery* **11**, 1874–1880.

CIGRÉ WG 33.04 1979 A critical comparison of artificial pollution test methods for HV insulators. *Electra* **64**, 117–136.

Claverie, P. & Porcheron, Y. 1973 How to choose insulators for polluted areas. *IEEE Trans. Power Apparatus Sys.* **92**, 1121–1131.

Comber, M. G. & Nigbor, R. J. 1982 Radio noise. In *Transmission line reference book, 345 kV and above*, 2nd edn, pp. 205–266. Electrical Power Research Institute.

Comber, M. G., Nigbor R. J. & Zaffanella L. F. 1982 Audible noise. In *Transmission line reference book, 345 kV and above*, 2nd edn, pp. 267–328. Electrical Power Research Institute.

Druez, J., Louchez, S. & Bouchard, G. 1990 Study of ice shedding phenomenon on cables. In *Proc. 9th Int. Conf. of Offshore Mechanics and Arctic Engineering, Houston, 1990*, no. 10296F, pp. 143–148.

EPRI 1982 *Transmission line reference book,* 345 kV *and above*, 2nd edn. Palo Alto: Electric Power Research Institute.

Erven, C. C. 1988 500 kV insulator flashovers at normal operating voltage. Presentation to the CEA Spring Meeting, Montreal.

Farzaneh, M. 1986 Contribution à l'étude des mécanismes des vibrations induites par effet de couronne. Thèse de doctorat d'état ès sciences, Université Paul Sabatier de Toulouse, France.

Farzaneh, M. 1991 Effect of ice thickness and voltage polarity on the flashover voltage of ice-covered high-voltage insulators. In *Proc. 7th Int. Symp. on High Voltage Engineering, August 1991, Dresden*, vol. 4, pp. 203–206.

Farzaneh, M. 1992 Effects of the intensity of precipitation and transverse wind on the corona-induced vibration of HV conductors. *IEEE Trans. Power Delivery* **7**, 674–680.

Farzaneh, M. & Drapeau, J. F. 1995 AC flashover performance of insulators covered with artificial ice. *IEEE Trans. Power Delivery* **10**, 1038–1051.

Farzaneh, M. & Kiernicki, J. 1995 Flashover problems caused by ice build-up on insulators. *IEEE Electrical Insulation Magazine* **11**, 5–17.

Farzaneh, M. & Kiernicki, J. 1997*a* Flashover performance of ice-covered insulators. *IEEE Can. J. Electrical Computer Engng* **22**, 95–109.

Farzaneh, M. & Kiernicki, J. 1997*b* Flashover performance of IEEE standard insulators under ice conditions. *IEEE Trans. Power Delivery* **12**, 1602–1613.

Farzaneh, M. & Laforte, J.-L. 1991 The effect of voltage polarity on ice accretions on short string insulators. *J. Offshore Mech. Arctic Engng* **113**, 179–184.

Farzaneh, M. & Laforte, J.-L. 1992 The effect of voltage polarity on icicles grown on line insulators. *Int. J. Offshore Polar Engng* **2**, 297–302.

Farzaneh, M. & Laforte, J.-L. 1994 Ice accretion on conductors energized by AC or DC: a laboratory investigation of ice treeing. *Int. J. Offshore Polar Engng* **4**, 40–47.

Farzaneh, M. & Melo, O. T. 1990 Properties and effect of freezing rain and winter fog on outline insulators. In *Cold regions science and technology*, pp. 33–46. Elsevier.

Farzaneh, M. & Melo, O. T. 1994 Flashover performance of insulators in the presence of short icicles. *Int. J. Offshore Polar Engng* **4**, 112–118.

Farzaneh, M. & Phan, L. C. 1984 Vibration of high voltage conductors induced by corona from water drops or hanging metal points. *IEEE Trans. Power Apparatus Sys.* **100**, 2746–2752.

Farzaneh, M. & Teisseyre, Y. 1988 Mechanical vibration of HV conductors induced by corona: roles of the space charge and ionic wind. *IEEE Trans. Power Delivery* **3**, 1122–1130.

Farzaneh, M., Kiernicki, J. & Drapeau, J. F. 1992 Ice accretion on energized line insulators. *Int. J. Offshore Polar Engng* **2**, 228–233.

Farzaneh, M., Kiernicki, J. & Martin, R. 1994 A laboratory investigation of the flashover performance of outdoor insulators covered with ice. In *Proc. 4th IEEE Int. Conf. on Properties and Application of Dielectric Materials, July 1994, Brisbane*, pp. 483–486.

Farzaneh, M., Bouillot, J., Teisseyre, Y., Svensson, E. C. & Dubouchet, P. 1996 Crystallographic structure of ice grown on an energized conductor. In *Proc. 7th Int. Workshop on Atmospheric Icing of Structures, June 1996, Chicoutimi*, pp. 351–354.

Farzaneh, M., Li, Y. & Zhang, J. 1997*a* Effects of altitude on AC flashover on ice surfaces. In *Proc. 10th Int. Symp. on High Voltage Engineering, August 1997, Montreal*, pp. 73–76.

Farzaneh, M., Li, Y. & Zhang, J. 1997*b* DC flashover performance of ice-covered insulators. In *Proc. 10th Int. Symp. on High Voltage Engineering, Montreal*, pp. 77–80.

Farzaneh, M., Zhang, J. & Chen, X. 1997*c* Modeling of the AC arc discharge on ice surfaces. *IEEE Trans. Power Delivery* **12**, 325–338.

Farzaneh, M., Bouillot, J., Teisseyre, Y., Svensson, E. C. & Donaberger, R. L. 1997*d* Structure of ice grown on high-voltage conductors. *Int. J. Offshore Polar Engng* **7**, 13–15.

Farzaneh, M., Li, S. Y. & Srivastava, K. D. 1998*a* Flashover on ice surfaces. *Atmospheric Res.* **46**, 37–47.

Farzaneh, M., Li, Y. & Zhang, J. 1998*b* DC flashover performance on ice surfaces at low atmospheric pressure. In *Proc. 8th Int. Workshop on Atmospheric Icing of Structures, June 1998, Reykjavik*, pp. 209–212.

Farzaneh, M., Zhang, J. & Chen, X. 1998*c* DC characteristics of local arc on ice surfaces. *Atmospheric Res.* **46**, 49–56.

Farzaneh, M., Brettschneider, S., Srivastava, K. D. & Li, S. Y. 1999*a* Impulse breakdown performance of the ice surface. In *11th Int. Symp. on High Voltage Engineering, August 1999, London*, vol. 4, pp. 341–344.

Farzaneh, M., Brettschneider, S., Srivastava, K. D. & Li, S. Y. 1999*b* Ultra-high-speed photographic observations of discharge development along the surface. In *11th Int. Symp. on High Voltage Engineering, August 1999, London*, vol. 3, pp. 297–300.

PHILOSOPHICAL TRANSACTIONS OF THE ROYAL SOCIETY A MATHEMATICAL, PHYSICAL & ENGINEERING SCIENCES

Fikke, S. M, Ohnstad, T. M., Telstad, T., Förster, H. & Rolfseng, L. 1994 Effect of long range airborne pollution on outdoor insulation. In *Proc. Nordic Insulation Symposium, June 1994, Vaasa*, paper 1.6, pp. 103–113.

Forrest, J. S. 1969 The performance of high-voltage insulators in polluted atmospheres. In *IEEE Conf. Paper No. 69 CP7-PWR, presented at the IEEE Winter Power Meeting, January 1969, New York.*

Fujimura, T., Naito, K., Hasegawa, Y. & Kawaguchi, K. 1979 Performance of insulators covered with snow or ice. *IEEE Trans. Power Apparatus Sys.* **98**, 1621–1631.

Ghosh P. S. & Chatterjee, N. 1996 Arc propagation over electrolytic surfaces under power frequency voltage. *IEEE Trans. Dielectrics Electrical Insulation* **3**, 529–536.

Godard, S. 1960 Mesure des gouttelettes de nuage avec un film de Collargol. Bulletin de l'Observatoire du Puy de Dôme, no. 2, pp. 41–46.

Goia, L. M. & Balan G. 1996 Romanian experience regarding operational behavior of HV OIs. In *Proc. 7th Int. Workshop on Atmospheric Icing of Structures, June 1996, Chicoutimi*, pp. 216–221.

Griffiths R. F. & Latham, J. 1974 Electrical corona from ice hydrometers. *Q. J. R. Met. Soc.* **100**, 163–180.

Havard D. G. & Pon, C. J. 1990 Use of detuning pendulums for control of galloping of single conductor and two- and four-conductor bundle transmission lines. In *Proc. 5th Int. Workshop on Atmospheric Icing of Structures, October 1990, Tokyo*, no. A7-4.

Havard D. G. & Pon, C. J. 1998 Galloping conductor control-status 1998. In *Proc. 4th Int. Workshop on Atmospheric Icing of Structures, September 1998, Paris*, pp. 314–318.

Hydro-Québec Committee of Experts 1998 January 1998 ice storm. Report for Hydro-Québec.

IEEE Working Group on Insulator Contamination 1979 Application guide for insulators in a contaminated environment. *IEEE Trans. Power Apparatus Sys.* **98**, 1676–1695.

International Electrotechnical Commission 1991 Artificial pollution tests on high voltage insulators to be used on AC systems. International Standard IEC 507.

Jones, K. F. 1993 The effect of horizontal and torsional coupling on vertical galloping. In *Proc. 6th Int. Workshop on Atmospheric Icing of Structures, September 1993, Budapest*, pp. 143–148.

Jordan J. B. & Saint-Arnaud, R. 1976 Electrical corona at ice surface. In *Proc. 4th Int. Conf. on Gas Discharges, September 1976, Swansea*, pp. 239–241.

Kannus, K., Verkonnen, K. & Lakervi, E. 1988 Effect of ice coating on the dielectric strength of high voltage insulators. In *Proc. 4th Int. Workshop on Atmospheric Icing of Structures, September 1988, Paris*, pp. 296–300.

Kannus, K., Lahti, K. & Nousiainen, K. 1998 Comparisons between experiments and calculations of the electrical behaviour of ice-covered high voltage insulators. In *Proc. 8th Int. Workshop on Atmospheric Icing of Structures, Reykjavik*, pp. 325–333.

Kawai, M. 1970 AC flashover test at project UHV on ice-coated insulators. *IEEE Trans. Power Apparatus Sys.* **89**, 1800–1804.

Khalifa, M. M. & Morris, R. M. 1968 Performance of line insulators under rime ice. *IEEE Trans. Power Apparatus Sys.* **86**, 692–698.

Lambeth, P. J. 1971 Effect of pollution on high voltage outdoor insulators. *IEEE Rev.* **118**, 1107–1130.

Larcombe, P. J., Kunda, W., Poots, G. & Elliott, J. W. 1991 Accretion and shedding of ice on cables incorporating free streamline theory and the joule effect. In *Proc. 3rd Int. Workshop on Atmospheric Icing of Structures, May 1986, Vancouver*, pp. 389–395.

Lee, L. Y., Nellis, C. L. & Brown, J. E. 1977 60 Hz tests on ice-coated 500 kV insulator strings. In *IEEE/PES Summer Meeting, July 1977, San Francisco*, paper A75-499-4.

Li, S., Zhang, R. & Tan, K. 1990 Measurement of dynamic potential distribution during the propagation of a local arc along a polluted surface. *IEEE Trans. Electrical Insulation* **25**, 757–761.

Meier, A. & Niggli, W. M. 1968 The influence of snow and ice deposits on super tension transmission line insulator string with special reference to high altitude operation. In *Proc. IEEE Conf., September 1968, London*, vol. 44, pp. 386–395.

Nasser, E. 1962 Zum Problem des Fremdschichtüberschlages an Insolatoren. *Elektrotech. Z.* A **83**, 356–365.

Nasser, E. 1972 Contamination flashover of outdoor insulation. In *Proc. Int. Symp. on High Voltage Engineering, 1972, Munich*, pp. 321-325.

Phan, C. L. & Laforte, J.-L. 1981 The influence of electrofreezing on ice formation on high voltage transmission lines. *Cold Regions Sci. Tech.* **4**, 15–25.

Phan, C. L. & Mansiaux, A. 1975 Corona and charge transfer on water drops in proximity of conductors. In *Proc. IEEE Summer Meeting, July 1975, San Francisco*, no. A-75-562-2, pp. 1–7.

Phan, C. L. & Matsuo, H. 1983 Minimum flashover voltage of iced insulators. *IEEE Trans. Electrical Insulation* **18**, 605–618.

Phan, C. L., Pirotte, P. & Trinh, N. G. 1974 A study of corona discharges at water drops over the freezing temperature range. *IEEE Trans. Power Apparatus Sys.* **93**, 724–734.

Phan, C. L., Laforte, J.-L. & Nguyen, D. D. 1983 The Lobe structure in ice accreted on an aluminium conductor in the presence of a DC electric field. *Ann. Glaciology* **4**, 228–235.

Poots, G. 1996 *Ice and snow accretion on structures*. Taunton: Research Studies Press.

Renner, P. E., Hill, H. L. & Ratz, O. 1971 Effects of icing on DC insulation strength. *IEEE Trans. Power Apparatus Sys.* **90**, 1201–1206.

Rizk, F. A. M. 1981 Mathematical models for pollution flashover. *Electra* **78**, 71–103.

Rizk, F. A. M. 1995 Review of the effect of pollution on high-voltage insulators and metal-oxide arresters. In *Proc. 9th Int. Symp. on High Voltage Engineering, August–September 1995, Graz*, pp. 9003-1–9003-10.

Roshan Fekr, M., McClure, G. & Hartmann, D. 1998 Investigation of transmission line failure due to ice shedding effects using dynamic analysis. In *Proc. 8th Int. Workshop on Atmospheric Icing of Structures, June 1998, Reykjavik*, pp. 11–16.

Sato, M., Saito, H., Kaga, A. & Akagami, H. 1989 Fundamental characteristics of AC flashover on contaminated insulators covered with ice. *Japanese J. Appl. Phys.* **28**, 889–896.

Schneider, H. M. 1975 Artificial ice tests on transmission line insulators—a progress report. In *Proc. IEEE/PES Summer Meeting, July 1975, San Francisco*, paper A75-491-1, pp. 347–353.

Shu, L., Sun, C., Zhang, J. & Gu, L. 1991 AC flashover performance of iced and polluted insulators for high altitude regions. In *Proc. 7th Int. Symp. on High Voltage Engineering, August 1991, Dresden*, vol. 4, pp. 303–306.

Shu, L., Sun, C., Zhang, J., Gu, L., Xiao, X. & Zhou, Z. 1993 AC flashover performance of iced insulators under pressure and pollution conditions. In *Proc. 8th Int. Symp. on High Voltage Engineering, August 1993, Yokohama*, paper 46.03, pp. 1–4.

Sklenicka, V. & Vokalek, J. 1996 Insulators in icing conditions: selection and measures for reliability increasing. In *Proc. 7th Int. Workshop on Atmospheric Icing of Structures, June 1996, Chicoutimi*, pp. 72–76.

Sklenicka, V., Hora, M., Korcova, I. & Vokalek, J. 1983 Influence of conductive ice on electric strength of HV insulators. In *Proc Int. Symp. on Pollution Performance of Insulators and Surge Diverters, December 1983, Madras*, vol. 1, pp. 1.02.01–1.02.05.

Soucy, L. 1996 Effet de la fonte et de la pollution sur la tension de tenue maximale des isolateurs recouverts de glace. Mémoire de maîtrise, Université du Québec à Chicoutimi.

Su, F. & Hu, S. 1988 Icing on overhead transmission lines in cold mountains district of southwest china and its protection. In *Proc. 4th Int. Workshop on Atmospheric Icing of Structures, September 1988, Paris*, pp. 354–357.

Su, F. & Jia, Y. 1993 Icing on insulator string of HV transmission lines and the harmfulness. In *Proc. 3rd Int. Offshore and Polar Engineering Conf., June 1993, Singapore*, pp. 655–662.

Sugawara, N., Hokari, K., Matsuda, K. & Miyamoto, K. 1990 Insulation properties of salt contaminated fog on structures. In *Proc. 5th Int. Workshop on Atmospheric Icing of Structures, October 1990, Tokyo*, no. B4-10, pp. 1–4.

Sugawara, N., Takayama, T., Hokari, K., Ito, S. & Yoshida, K. 1993 Effect of icicle growth of hard rime accreted insulators on withstand voltage. In *Proc. 8th Int. Symp. on High Voltage Engineering, 1993, Yokohama*, vol. 2, pp. 157–160.

Teisseyre, Y. & Farzaneh, M. 1990 On the mechanism of the ice accretion on HV conductors. *Cold Regions Sci. Tech.* **18**, 1–8.

Tymofichuk, T. E. 1986 A utility's recent experiences with devastating ice storm and a program in response. In *Proc. 3rd Int. Workshop on Atmospheric Icing of Structures, Vancouver, May 1986*, pp. 469–480.

Udo, T., Watanabe, Y., Mayumi, K., Ikeda, G. & Okada, T. 1968 Switching surge flashover characteristics of long insulators strings and stacks. CIGRE Paper 25-04.

Vuckovic, Z. & Zdravkovic, Z. 1990 Effect of polluted snow and ice accretions on high-voltage transmission line insulators. In *Proc. 5th Int. Conf. on Atmospheric Icing of Structures, October 1990, Tokyo*, no. B4-3, pp. 1–6.

Vuckovic, Z., Plazinic, S. & Nikolic, I. 1996 Failures of overhead lines due to ice and wet snow in a part of Balkan peninsula (Serbia). In *Proc. 7th Int. Workshop on Atmospheric Icing of Structures, June 1996, Chicoutimi*, pp. 210–215.

Wareing, J. B. & Bracey, R. H. 1998 Failure mechanisms in wood poles under severe conductor ice loading. In *Proc. 8th Int. Workshop on Atmospheric Icing of Structures, June 1998, Reykjavik*, pp. 35–41.

Watanebe, Y. 1977 Flashover tests of insulators covered with ice or snow. *IEEE/PES Summer Meeting, July 1977, San Francisco.* paper F77-570-5.

White, H. J. 1962 *Industrial electrostatic precipitation.* Reading, MA: Addison-Wesley.

Wilkins, R. 1969 Flashover voltage of high-voltage insulators with uniform surface-pollution films. *Proc. IEE* **116**, 457–465.

Wu, D., Halsan, K. A. & Fikke, S. M. 1996 Artificial ice tests for long insulator strings. In *Proc. 7th Int. Workshop on Atmospheric Icing of Structures, June 1996, Chicoutimi*, pp. 67–71.

Yamazaki, T., Takino, Y., Matsuoka, R. & Ito, S. 1993 Flashover voltage characteristic of contaminated station insulators under temporary AC overvoltages in the AC system connected with frequency converter station. *Electrical Engng Japan* **113**. (Transl. *Denbi Gakkai Ronbunshi* 1992 **112-B**.)

Zhang, J. & Farzaneh, M. 2000 Propagation of AC and DC arcs on ice surfaces. *Trans. Dielectrics Electrical Insulation* **147**, 81–86.